DOE/PC/93217--T9

FINAL TECHNICAL REPORT

Superior Catalysts for Selective Catalytic Reduction of Nitric Oxide

October 1, 1993 - September 30, 1995

by

R. T. Yang, W. B. Li, J. P. Chen, M. C. Hausladen, L. S. Cheng, and E. S. Kikkinides

Department of Chemical Engineering
State University of New York at Buffalo
Buffalo, NY 14260

and

Department of Chemical Engineering
University of Michigan
Ann Arbor, MI 48109

Submitted to

Pittsburgh Energy Technology Center
U. S. Department of Energy
under Contract DE-FG22-93PC932217

TABLE OF CONTENTS

SUMMARY

The most advanced and proven technology for NO_x control for stationary sources is Selective Catalytic Reduction (SCR). In SCR, NO_x is reduced by NH_3 to N_2 and H_2O. The commercial catalysts are based on V_2O_5/TiO_2, and the vanadium-based catalysts are patented by the Japanese (Mitsubishi). However, there are three main disadvantages for the vanadium-based SCR catalyst:

(a) A tendency to be poisoned in the flue gas

(b) Oxidation of SO_2 to SO_3 by V_2O_5. This is a particularly severe problem due to the higher sulfur content of American coals compared with coals used in Japan (from Australia) and in Europe.

(c) Environmental problems involved in the disposal of the spent catalyst (due to the toxicity of vanadium).

In order to overcome these problems, in addition to the undesirable dominance by the Japanese patent position, we have studied in this project a new type of catalyst for the SCR reaction; namely, pillared clays, which have adjustable, unique structures and acidity. Three types of catalysts were developed and tested for this reaction, i.e. Fe_2O_3-pillared clays, delaminated Fe_2O_3-pillared clays, and ion-exchanged pillared clays. The project was divided into sixteen tasks, and will be reported as such.

In Task 1, a new SCR reactor system was designed and built. Besides a chemiluminescent NO/NO_x analyzer, the new SCR reactor system had an on-line quadrupole mass spectrometer for N_2O analysis and an on-line GC for N_2 product monitoring, while SO_3 was collected and analyzed by using a wet analytical technique. The schematic diagram of the experimental SCR reactor is shown in Fig. 1.

In Task 2 and Task 3, Fe_2O_3-pillared clays were developed for SCR of NO with ammonia as the reducing agent. In Task 2, a general procedure for the synthesis of stable Fe_2O_3-pillared clay was established. The chemical composition of the Fe_2O_3-pillared clays were analyzed by inductive coupled plasma spectrometric analysis (ICP). The preliminary results for promoters in the SCR Fe_2O_3-pillared clay catalyst are described in Task 3. The results showed that the activities were near that of commercial V_2O_5/TiO_2 catalysts. Moreover, the SO_2 - SO_3 conversion was substantially lower with the pillared clay catalyst, which could be an important advantage. The results are shown in Fig. 2 and Fig. 3.

Task 4 to Task 13 were focused on a more active catalyst; that is, delaminated Fe_2O_3-pillared clays which showed no distinct XRD pattern and were different from Fe_2O_3-pillared clays. In Task 4 a delaminated Fe_2O_3-pillared clay was synthesized. The structural changes in the clay were characterized by x-ray diffraction techniques (XRD), as shown in Fig. 5. The XRD analysis showed that the delaminated sample lost not only its (001) diffraction, but also the two-dimensional diffraction peaks at d-pacings equal to 4.49 Å and 2.57 Å, i.e. the clay lost its two-dimensional characteristic diffraction. As discussed by Occelli et al. (8), the delaminated clay does not preclude the possibility of short range ordering in the interlayer direction. Also the absence of the two-dimensional reflections does not mean that there was no short range two-dimensional structure in the clay. Rather, the large two-dimensional structure could have been fragmented into small pieces giving a semi-amorphous form. These small pieces would be the basic units in the structure referred to as "house-of-cards," which have shown to be superior over the normal pillared clays in many aspects (7,8,9,10,11).

In Task 5, the selective catalytic reduction activities of the delaminated pillared clay were tested and compared with four other most active SCR catalysts; a commercial V_2O_5 + WO_3/TiO_2 catalyst, an Fe_2O_3-pillared clay, and two supported Fe_2O_3 catalysts (on Al_2O_3 and

TiO_2). The delaminated Fe_2O_3-pillared clay exhibited the highest SCR activities (Fig. 7). Catalyst stability tests showed that the delaminated sample was also stable.

In Task 6, deactivation effects of SO_2 and H_2O on the SCR activities of the delaminated Fe_2O_3-pillared clay were studied, and compared with other SCR catalysts. The delaminated clay catalyst showed the least deactivation (Fig. 9).

In Task 7, effects of synthesis conditions on the delaminated Fe_2O_3-pillared clay were studied. Since the synthesis of this PILC was undertaken under a specific set of conditions and it was known that the PILC properties depended strongly on the synthesis conditions, we then proceeded to examine in a systematic manner the dependence of the catalytic properties of the PILC on its synthesis conditions. Four parameters in the synthesis were studied: Fe precursors, pH of the pillaring solution, concentration of the pillaring solution, and the starting clay.

In Task 8, the promoting effects of Cr_2O_3 on SCR activity were studied. A strong promoting effect at 300°C (by doping 2.5% Cr_2O_3 in the delaminated PILC) was seen. The results are shown in Fig. 10.

In Task 9, the effects of several significant parameters (reaction temperature, oxygen concentration, and internal diffusion) on the SCR of NO with NH_3 on delaminated Fe_2O_3-pillared clay were studied and the results are shown in Fig. 11 and Fig. 12. Moreover, the promoting effects of Ce, Cu and La oxides on the pillared clay catalyst performance were investigated and are shown in Fig. 13. The results showed that addition of La_2O_3, CuO and CeO_2 increased the activities of the delaminated Fe_2O_3-pillared clay catalyst. Cerium, in particular, has a strong promoting effect on NO conversion.

In Task 10, the poisoning effects of alkali metals (as Na_2O, K_2O and Cs_2O) on the delaminated pillared clay catalyst for SCR of NO with NH_3 were studied and the results are shown in Fig. 14. The results showed that the catalyst activity decreased with both Na_2O and K_2O at all temperatures between 250° and 400°C. The Cs_2O dopant also decreased the NO conversion at reaction temperatures below 350°C. However, when the reaction temperature reached 400°C, the NO conversion actually increased to 85% compared to 78% without the addition of Cs_2O. It seemed that the very strong electron donating ability of cesium played a role in the SCR activity. A redox mechanism might be functional in NO reduction of the Fe-Bentonite pillared clay catalyst. The addition of cesium may have accelerated the redox process on the catalyst surface.

At higher temperatures (300°C - 400°C), the very active Cs_2O (resulting from its strong electron donating ability) migrated and dispersed better, which led to a change on the surface. This change promoted the adsorption and reaction of NH_3 and/or NO on the catalyst surface, hence the SCR activity.

In Task 11, the effects of sulfur dioxide and water vapor on the performance of the high activity catalyst, that is Ce-doped Fe-Bentonite pillared clay (Ce-Fe-Bentonite), were examined and are shown in Fig. 15. The results showed only slight decreases in NO conversion upon adding 1000 ppm SO_2 and 5% H_2O at 350°C-400°C. For example, at 350°C NO conversion decreased only from 90% to 86%. These results suggest that the Fe-Bentonite pillared clay doped with cerium oxide is an effective SCR catalyst that is resistant to sulfur dioxide and water vapor at the practical temperature range of 350°C-400°C.

In Task 12, the delaminated Fe_2O_3-PILC catalyst was characterized by micropore probing through adsorption measurements (Fig. 18), Mossbauer spectroscopy (Fig. 16) and IR spectroscopy (Fig. 19-Fig. 21). The Mossbauer spectroscopy and molecular probing results indicated that the structure of the delaminated sample could be described as "house of cards,"

which is consistent with XRD results. *In situ* FT-IR results showed that the origin of the strong Bronsted acid sites in this clay catalyst was probably due to interactions between Fe_2O_3 and the clay.

In Task 13, TPD (temperature programmed desorption) techniques were employed to study the reaction mechanism of the selective catalytic reduction of NO with ammonia over the iron oxide pillared clay catalyst (Fig. 22 - Fig. 25). From the TPD results for the Fe_2O_3-PILC catalyst, it was seen that a significant amount of NO_x was chemisorbed at temperatures up to 600°C, i.e. well above the SCR reaction temperature of 350°C-400°C. It is, therefore, reasonable to conclude that SCRT reaction on the Fe_2O_3-PILC follows a different type of mechanism, i.e. that of the Langmuir-Hinshelwood type, involving both chemisorbed NO_x and NH_3 (or NH_x).

In Task 14 to Task 16, exploratory work was done on using ion exchanged pillared clays for SCR. The idea was to minimize pore diffusion limitation of the delaminated Fe_2O_3-pillared clays. In Task 14, an iron ion-exchanged titania pillared clay (Ti-PILC) was prepared and its catalytic activity for the SCR of NO with NH_3 was studied, which showed a high activity and a high SO_2 and H_2O resistance at high temperatures (i.e. above 400°C) (Fig. 26).

In Task 15, a sulfur dioxide resistant catalyst, Fe_2O_3/TiO_2, for the SCR of NO with ammonia by doping Fe_2O_3 on a high surface area TiO_2 support was made by the sol-gel route. The purpose of this work was also to overcome the intracrystalline diffusion limitation of delaminated Fe_2O_3-pillared clay catalyst for SCR of NO with ammonia. The interesting results were that the Fe_2O_3/TiO_2 catalyst was strongly resistant to sulfur dioxide. This is an important result for application to high sulfur American coals.

In the last task, Task 16, we explored the possibility of using pillared clays (and ion exchanged pillared clays) for the SCR of NO by a class of more desirable reducing agents, hydrocarbons. The latter is more desired as explained below. Selective catalytic reduction of NO by NH_3 is presently performed with vanadia-based catalysts for flue gas applications. Hydrocarbons would be the preferred reducing agents over NH_3 because of the practical problems associated with the use of NH_3 (i.e. handling and slippage through the reactor). SCR of NO by hydrocarbons can also find important applications for lean-burn (i.e. O_2-rich) gasoline and diesel engines where the noble-metal three-way catalysts are not effective in the presence of excess oxygen. The results from the SCR of NO with ethylene over Cu^{2+} ion exchanged TiO_2 pillared clay were illustrated in Fig. 27 and Fig. 28.

Figure 27 shows that the catalytic activity increased with increasing temperature, reaching a maximum of 79% NO conversion at 300°C, and then decreased at higher temperatures. It is clear that the Cu^{2+} exchanged TiO_2-PILC is substantially more active than the Cu-ZSM-5 catalyst. In the presence of H_2O (5%) and SO_2 (500 ppm), the activities of Cu^{2+}-exchanged TiO_2-PILC decreased, as expected. However, these decreased activities were still higher than that of Cu-ZSM-5 under SO_2/H_2O-free conditions (Fig. 27). The C_2H_4 SCR activities of the Ce-doped catalyst are shown in Fig. 28. The ceria dopant increased the C_2H_4 SCR activity at temperatures higher than 300°C, but decreased the activity at 250°C. The effect of $SO_2 + H_2O$ on the activity of the Ce-doped catalyst is also shown in Fig. 28, where a decrease but a still high activity was seen. The catalytic activities were fully recovered after SO_2 and H_2O were switched off. Thus, SO_2/H_2O did not alter (or poison) the active sites; rather, they probably occupied the sites reversibly.

Task 1. SCR Reactor Construction and Upgrading

The SCR reactor system that was used in our laboratory for an earlier EPRI program was dedicated to this program. The reactor system consisted of a chemiluminescent NO/NO_x analyzer (Thermo Electron Corporation Model 10) and is shown in a schematic diagram in Figure 1. This reactor system did not have the capability for N_2O and SO_3 analyses. N_2O could not be detected by the chemiluminescent analyzer. The emission of both N_2O (which is very stable) and SO_3 from SCR were of serious concern, especially for application to power plants using high sulfur American coals.

In order to upgrade the reactor system for N_2O and SO_3 analyses, and also to enable us to produce more experimental results, it was decided to build another SCR reactor system. The rebuilt SCR reactor system had an on-line quadrupole mass spectrometer for N_2O analysis while the SO_3 was collected and analyzed by using a wet analytical technique. Also on-line was a GC for N_2 product monitoring. The rebuilt reactor system is described below.

The tubular reactor was made of quartz heated by a coiled Nichrome wire. The reactor temperature was controlled by a programmable temperature controller (Omega CN-2010). The catalyst was supported on a fritted quartz support.

The simulated flue gas was made by mixing the gaseous reactants. The flow rates of the reactants were controlled by two sets of flow meters. Rotameters were used to control flows with high flow rates (i.e. He, NH_3/He, NO/He); mass flow meters were used for gases with low flow rates (SO_2 and O_2). The pre-mixed gases (0.8% NO in He and 0.8% NH_3 in He) were supplied by Cryogenic Supply. The 8% water vapor was generated by passing helium through a heated gas-washing bottle containing distilled water. All tubings leading to the reactor were heated tapes in order to prevent the deposition of ammonium sulfate. The effluent was analyzed by an on-line GC for N_2. From the N_2 concentration, the NOx Æ N_2 conversion was known. A quadrupole mass spectrometer (UPI Model 1000) was also available to spot check the N_2O concentration in the product. (Attempts to analyze N_2O by GC with Porapak Q and R columns had failed, thus we had to resort to mass spectroscopy.)

SO_3 Analysis. A wet analytical technique for measuring SO_3 concentration was established. The procedure is described as follows. The effluent from the SCR reactor was bubbled through a $BaCl_2$ solution, where the SO_3 was captured quantitatively. The $BaSO_4$ formed a precipitate in the form of a white powder. The precipitate was collected on an ashless filter paper, which was then burned along with the precipitate in a crucible, so the amount of the precipitate could be accurately weighed. Heating of the effluent up to the point of collection was provided, so the formation of $(NH_4)_2SO_4$ in the lines was avoided. This technique was tested successfully in our laboratory. A dummy catalyst was used in the control experiment. In a preliminary SCR run with the Fe_2O_3-pillared clay catalyst, an SO_2-to-SO_3 conversion of 0.5% was obtained, which was lower than those with the V_2O_5/TiO_2 catalysts reported in the literature. This was an encouraging result, since the SO_2 Æ SO_3 conversion was an important issue for the SCR reaction.

Task 2. Iron Oxide Pillared Clay Synthesis.

The general procedure for preparing pillared clays is described below:

(1) A clay sample was suspended in distilled water.

(2) A polymeric (or oligomeric) cation complex was prepared by dissolving a metal salt in distilled water. If necessary, a base was added into the solution to promote the hydrolysis. The solution was aged at a selected temperature for a period of time.

(3) By mixing the clay suspension and the polyoxometallic complex solution, the ion exchange reaction took place.

(4) After a certain period of ion exchange at a given temperature, the clay sample was collected by filtration or centrifuge, followed by heating (e.g. to 400°C) to decompose the polyoxometallic complex into oxide which forms pillars.

Fe_2O_3-pillared interlayer clay (Fe_2O_3-PILC could be prepared by ion exchange of smectite (especially montmorillonite) with iron cation containing compounds, such as a solution

of any of the iron salts $Fe(NO_3)_3$, $FeCl_3$, $Fe(ClO_4)_3$, $Fe_2(C_2O_4)_3$, $Fe_2(SO_4)_3$ and iron organometallic compounds.

It has been reported in the literature that the most stable Fe_2O_3-PILC was prepared by intercalating with an aqueous solution of trinuclear acetato hydroxyl-iron(III) nitrate, $[Fe_3(OCOCH_3)_7OH \cdot 2N_2ONO_3]$. Therefore, the above iron acetate was chosen as a first candidate for Fe_2O_3-PILC preparation.

A. Preparation of Trinuclear Acetato Hydroxyl-Iron(III) Nitrate

One hundred grams of iron nitrate, $Fe(NO_3)_3 \cdot 9H_2O$ (Strem Chemical, Inc.) was dissolved in 50 ml ethanol (Fisher Scientific Co.). The solution was stirred until iron nitrate was completely dissolved. 140 ml of anhydrous acetic acid (99.9%, J. T. Baker Inc.) was added to the stirred solution. A very dark solution was observed as soon as the acetic acid solution was added. The solution was stirred 5 more minutes and then was kept in an ice bath for precipitation. The resulting precipitation or crystalline (trinuclear acetato hydroxyl-iron nitrate) was collected by vacuum filtration or heated on a hot plate to evaporate ethanol and NHO_3. The collected precipitate was used as the pillaring agent without further purification.

B. Preparation of Fe_2O_3-PILC

The collected trinuclear acetato hydroxyl-iron(III) nitrate crystal was dissolved in two liters of distilled water. 20 grams of bentonite (Fisher Scientific) was added into the stirred solution. After reacting (ion exchanging) for at least four hours, the suspension solution was kept still to separate clay from the solution. The prepared sample was first dried at 120°C for 24 hrs, then crashed and sieved to collect the desired fractions. The sample was further heated to 400°C at a rate of 2°C/min. in a tubular reactor and was kept at that temperature for a period of at least 12 hours.

C. Chemical Composition Analysis

To precisely and accurately analyze the chemical constitutions of the clay and the prepared pillared clay, inductive coupled plasma spectrometric analysis (ICP) was performed in this work. (This was done in the Chemistry Department at SUNY). The sample must be first dissolved into a solution. Because of the existence of sodium in the clay sample, instead of using the standard procedure whereby the sample mineral is fused with Na_2CO_3 followed by dissolving in water, a now more widely used method is adopted where the clay is fused with lithium borates followed by dissolution. It is found that this is an excellent technique for bringing silicates into solution for ICP or atomic absorption analysis. The chemical compositions of the clay and the pillared clay were analyzed by using a model Thermo Jarrel Ash 61 ICAP analyzer. The clay sample (0.1000 gram) was mixed with 0.600 g total of lithium metaborate and lithium tetraborate (1:2 ratio and fused) in a graphite crucible at 1000°C for about one hour. After slowly cooling to room temperature, the fluxed bead was dissolved in 250 ml hot 2% HNO_3 solution. When the fluxed bead completely dissolved, the solution was filtered to remove graphite fiber impurity that came from the crucible.

The ICP analysis results are shown in Table 1. The water contents in Table 1 were analyzed separately by thermo-gravimetric analysis (TGA) by heating the samples in helium to 400°C and measuring the weight loss.

Table 1 shows that after ion exchange/pillaring reaction, the compositions of the cations, Na^+, K^+, CA^{2+}, and Mg^{2+} all decreased. However, the most significant change in the synthesized sample was the increase in the iron oxide content from 3.66% to about 10%.

Task 3. SCR Activity of Fe_2O_3-PILC

The SCR activity of Fe_2O_3-PILC was measured via NO_X conversion expressed by

$$\text{NO Conversion} = X = \frac{[NOx]_{in} - [NOx]_{out}}{[NOx]_{in}}$$

The rate constant was calculated assuming plug flow reactor. The catalyst activity was expressed by a first order rate constant (k) with respect to NO,

$$\text{Rate} = -\frac{1}{W}\frac{d[NO]}{dt} = k[NO]^1[NH_3]^0$$

where W is the weight of the catalyst. Assuming plug flow, the rate constant (k) can be calculated by:

$$k = \frac{F_0}{[NO_0]W}\ln(1-X)$$

where F_0 is the inlet molar flow rate of NO, $[NO]_0$ is the inlet molar concentration of NO, and x is the fractional NO conversion.

SCR rates on the Fe_2O_3-PILC catalyst were measured at 4 temperatures and under the following conditions:

- With H_2O and SO_2 (indicated by $+H_2O$, $+SO_2$)
- With H_2O and without SO_2 (indicated by $+H_2O$, $-SO_2$)
- Without H_2O and SO_2 (indicated by $-H_2O$, $-SO_2$)

In order to obtain an accurate reading from the NO_x chemiluminescent analyzer, the NO_x conversion was kept low by using a very high space velocity. (Here the space velocity is expressed by gas hourly space velocity, i.e. the number of reactor volumes of reactant gas at the ambient conditions processed per hour.) The experimental results are shown in Figures 2 and 3. The space velocity was 30,000 hr^{-1}, which was a very high space velocity. The rate constant at 400°C was 22.5 ml/g/s under SO_2/H_2O-free conditions (Figure 3). This rate constant was quite high; the rate constant for the commercial $V_2O_5/WO_3/TiO_2$ catalyst is about 40 ml/g/s. It is quite encouraging that the first Fe_2O_3-PILC sample showed this level of activity. However, like

the commercial catalyst, H_2O has a negative effect while the effect of SO_2 is small. The lack of SO_2 effect is encouraging.

Task 4. Iron Oxide Pillared Clay Synthesis

1. Synthesis of Delaminated Pillared Clay

The clay suspension solution was prepared by dispersing 10 grams of bentonite (Fisher Scientific, purified grade) in 1 liter distilled water. Our chemical analysis showed that the bentonite from Fisher was mostly Na^+ montmorillonite. The pillaring agent was prepared by hydrolysis of 3 liters of 0.2 M $Fe(NO_3)_3$, and anhydrous sodium carbonate was added to the vigorously stirred ($Fe(NO_3)_3$ solution to adjust the pH value of the solution. CO_2 evolution occurred during hydrolysis. The resulting solution was aged for 24 hours at room temperature prior to use. The ratio of base to iron was equal to 2, i.e. $OH^-/Fe = 2$, and the final pH value of the solution was 1.8. The aqueous clay suspension was added by drops to the polyoxoiron cation solution through a funnel. The cation exchange capacity of the bentonite was 103 meq/100g. The ratio of Fe/clay was approximately 60 (mmole of Fe)/m.e.q. of clay). The pillaring/delaiminating (ion-exchange) reaction took place at room temperature. It was found that the nature of the pillared clay product depended on the reaction condition. Pillared clay resulted from short (e.g. below 3 hrs.) reaction times whereas delaiminated pillared clay formed after long reaction times (e.g. over 12 hrs.). (The delamination process in this reaction is under further study.) Both Fe_2O_3-PILC and delaminated Fe_2O_3-PILC were prepared and were subsequently subjected to SCR activity tests. After the reaction, the suspension solution was kept still to separate the top portion of the clear solution. The pillared/delaminated clay was separated by vacuum filtration of the suspension solution. The collected solid sample was redispersed and washed in distilled water. The final sample was collected after repeated dispersion/washing/filtration, i.e. three times. The collected solid samples were first dried at 120°C for 24 hours, then crushed and sieved to collect the desired fractions. The samples were further heated to 400°C at a rate of 2°C/min in a tubular reactor and were kept at that

temperature for a period of at least 12 hours. After these pretreatments, the samples were ready for further experiments.

2. Chemical Composition Analysis

The chemical composition of the delaminated pillared clay was analyzed by inductively coupled plasma (ICP) atomic emission spectrometer (Thermo Jarrel Ash 61 ICAP). A fusion-dissolution method was used for sample preparation. The clay sample (0.1 gram) was fused with a mixture (0.6 gram total) of lithium metaborate and lithium tetraborate (at a weight ratio of 1:2) in a graphite crucible at 1000°C for about one hour. After slowly cooling to room temperature, the fluxed bead was dissolved in 250 ml hot 2% HNO_3 solution. When the fluxed bead dissolved completely, the solution was filtered to remove graphite fiber impurity that came from the crucible. The bentonite sample was analyzed by the same procedure.

The ICP results are shown in Table 1. The water contents in Table 1 were obtained separately by thermo-gravimetric analysis (TGA) by heating in helium to 400°C. ICP results of montmorillonite and Fe_2O_3-PILC have been reported in a previous quarterly report. They are included here for comparison.

Table 1 shows that after ion exchange/pillaring reaction, the contents of the cations Na^+, K^+, Ca^{++}, and Mg^{++} decreased. However, the most significant change in the synthesized samples was the iron oxide content, which increased from 3.66% to up to 30.61%. The iron oxide pillared clay contained about 10% iron oxide. The extra amount of iron oxide in delaminated/pillared clay was doped on the surface.

3. X-Ray Diffraction Characterization

X-ray diffraction patterns were obtained using powder samples in a Stoe transmission powder diffractometer with CuKα radiation. Normally, the data were collected in 2 minutes. For samples with weak signals or being amorphous, the data collection time was extended to at least six minutes.

XRD was also used to determine the Fe_2O_3 particle size. The particle size measurement was based on X-ray line broadening using a method described by Klug and Alexander (1). Silicon was used as a standard for calibration of half-height line width.

3A. Structural Analysis by X-Ray Diffraction

X-ray diffraction (powder) patterns of the starting clay (bentonite) are shown in Figure 4. Pattern A was recorded without pre-treatment. Pattern B was recorded after the sample was calcined at 300°C for two hours. The decrease of d_{001} spacing from 12.1Å to 9.85Å was due to dehydration of the interlayer hydrates.

XRD patterns of smectite clays generally show basal diffraction *001* and two-dimensional diffraction *hk* only (2,3). Other *hkl* diffractions are usually not observed. The random or unoriented clay samples only show a strong *001* diffraction; the *hk* diffractions are also strong but diffusive (Fig. 4). The characteristics of the *hk* diffractions is that the peak terminates steeply at the low-angle side but falls off gradually at the high-angle side. The *hk* reflections are characteristic of the type of the clay mineral, whereas the (001) basal reflection is characteristic of the conditions, i.e. interlayer water, cations, etc.

Other major peaks in Fig. 4 are assigned as follows (4). The peaks at 2θ of 19.6° (d = 4.49Å) and 34.9° (d = 2.57Å) are assigned to the two-dimensional diffraction, *hk*, reflections. These non-basal *hk* two-dimensional reflections arise from the diffraction of the random stacking of layers. Each observed *hk* two-dimensional reflection is the summation of several *hk* index pairs. The diffraction at 19.6° (d = 4.49Å) is the summation of *hk* indices of (02) and (11), and the diffraction at 34.9° (d = 2.57Å) is the summation of *hk* indices of (13) and (20). The two-dimensional *hk* reflections are strongest in unoriented crystals. The peak at 2θ = 26.5° (d = 3.36Å) is the diffraction of (101) from quartz impurity.

The XRD patterns of the synthesized clay catalysts are shown in Fig. 5. In the Fe_2O_3-pillared clay sample, the d_{001} spacing was 26.4Å, and the two-dimensional *hk* reflections remained. For the delaminated sample, no reflections were observed in the 2θ range 3°-45°. The

disappearance of the regular basal spacing of clay and the distinct lines corresponding to larger interlayer spacing (i.e. $2\theta<5°$) was also observed by Burch and Warburton (5) in their preparation of Fe_2O_3 pillared clay. Pillared clays that exhibit no (001) reflection have been referred to as "delaiminated clay" (6,7) in the literature.

The XRD analysis showed that the delaminated sample not only lost its (001) diffraction, but also the two-dimensional diffraction peaks at d-pacings equal to 4.49Å and 2.57Å, i.e. the clay lost its two-dimensional characteristic diffractions. As discussed by Occelli et al. (8), the delaminated clay does not preclude the possibility of short range ordering in the interlayer direction. Also the absence of the two-dimensional reflections does not mean that there was no short range two-dimensional structure in the clay. Rather, the large two-dimensional structure could have been fragmented into small pieces giving a semi-amorphous form. These small pieces would be the basic units in the structure referred to as "house-of-cards," which have shown to be superior over the normal pillared clays in many aspects (7,8,9,10,11).

3B. Fe_2O_3 Particle Size by XRD Line Broadening

Thechemical composition analysis indicated that there were Fe_2O_3 particles in addition to the fragmented Fe_2O_3-pillared clay. The Fe_2O_3 particle size has been analyzed by XRD and plans are under way for Mossbauer analysis.

As discussed, the x-ray diffraction patterns for the clay structure disappeared. However, the weak and broadened peaks at 2θ of 33.36° (d = 2.686Å) and 35.79° (d = 2.520Å) became discernible by extending the data collection time to 400 seconds, as shown in Fig. 6. These two peaks were reflections by the (104) and (110) faces, respectively, of hematite (12).

From the line broadening, the particle size can be calculated with the following formula (1).

$$L = K\lambda / \beta\cos\theta$$

where L is the mean dimension of the crystallites, K is the Scherrer constant and for spheres, K = 0.893 ($\beta_{1/2}$), λ is the wavelength of CuKα which is 1.5418Å, β is the breadth (line width at half height, $\beta_{1/2}$) of pure diffraction profile on 2θ scale in radians, and θ is the diffraction angle.

The value of b was calculated by the following procedure (1): By using the breadths of silicon standard (b_0) and catalyst sample (B_0) from their XRD profiles and finding the Kα doublet separation of Cu radiation from the literature, the corrected breadths of silicon standard (b) and catalyst sample (B) were obtained. With the ratio of b/B and β values was found from the curves for correction integral breadths of Debye-Scherrer lines for instrumental broadening. The value of β was found to be 0.6163. Therefore, the average α-Fe_2O_3 particle size was 170 Å.

Task 5. SCR Activity and Stability

1. Activity for Selective Catalytic Reduction of NO by NH_3

The NO SCR activities for the delaminated Fe_2O_3-pillared clay were measured under conditions both with and without SO_2/H_2O. The results are shown in Figs. 4 and 5. Three other high-activity catalysts were also included for comparison: $V_2O_5 + WO_3/TiO_2$, Fe_2O_3/Al_2O_3 and Fe_2O_3/TiO_2. The delaminated pillared clay showed clear superiority over the other catalysts.

The $V_2O_5 + WO_3/TiO_2$ contained 8.2% WO_3 and 4.8% V_2O_5. This is a catalyst being commercially used (13,14) and its SCR activity was the same as a US commercial catalyst tested in our laboratory. This catalyst was SO_2 resistant. However, the delaminated pillared clay exhibited higher activities under conditions both with and without SO_2/H_2O. The NO conversions at 400°C for this catalyst reached 98.8% (without SO_2/H_2O) and 98.7% (with SO_2/H_2O). Its activity was decreased considerably at lower temperatures.

Supported Fe_2O_3 catalysts were among the most active catalysts for the NO SCR reaction (15). The data by Wong and Nobe were also included for comparison, Fig. 4. Wong and Nobe only studied the reaction without SO_2 and H_2O, and their reactant gas composition was the same as that used in this study. Their catalyst amount was 14 g and the gas flowrate was

300 INTP/hr. So a conversion, based on first-order reaction (15) and plug flow reactor, was needed for our comparison. The conversions shown in Fig. 7 were with this conversion. It is seen that the supported Fe_2O_3 catalysts show lower activities than Fe_2O_3-pillared clay, as well as the other catalysts. It was noted by Wong and Nobe that there was pore diffusion limitation in their reactions, and effectiveness factors ranging from 16% to 95% were indicated. By including the effectiveness factor, however, the NO conversion for the delaminated pillared clay was still higher than the supported Fe_2O_3 catalysts.

2. Catalyst Stability

The stability of iron oxide pillared clays have been studied by a number of researchers. It was reported that sulfite-pillared clay was stable at elevated temperatures and pressures and iron oxide pillared clay was stable under reducing conditions even at a temperature as high as 500°C. However, unstable iron oxide pillared clays have also been observed. SEM/EDS analysis (16) showed that the iron oxide pillars migrated to the edge of the clay when the pillared clay was exposed to air at ambient temperature for three months. Prompted by these reports, the delaminated pillared clay was subjected to a longevity test under the SCR conditions. As shown in Table 2, the NO conversion stayed in the range 83%-86% when SO_2 and H_2O were switched on, and the conversion was stable at 95%-99% without SO_2 and H_2O. No deactivation was shown after four days. The delaminated clay is therefore stable under the SCR reaction conditions.

Task 6. Poison Resistance Study

To understand the poison resistance of the delaminated Fe_2O_3-PILC, the catalyst was tested under both without SO_2/H_2O and with SO_2/H_2O conditions at temperatures from 250°C to 400°C. The results of SCR activities with SO_2 and H_2O are shown in Fig. 8. For the delaminated pillared clay, the activities are compared for conditions with and without H_2O/SO_2, Fig. 9. Figure 9 shows that at lower temperatures (<300°C), SO_2/H_2O exhibited a deactivation

effect on the SCR activity, this deactivation effect decreases as the reaction temperature approaches the normal SCR reaction temperature (i.e. 400°C). At 400°C, the negative effect of SO_2/H_2O almost totally disappeared.

Task 7. Effects of Synthesis Conditions on the PILC Catalyst - Search for the Best Catalyst

The most important step in the synthesis of metal oxide pillared/delaminated clay is ion-exchange. Poly- or oligometric hydroxy metal cations are exchanged with the interlayer cations of clay, and then these hydroxy-metal cations are decomposed into oxide pillars between the silicate layers by heat treatment.

The hydrolysis conditions to form oligomers from the pillaring solution and the intercalation conditons to substitute the oligomers for the small cations between the layers are very important to the final PILC.

In this task, the experimental results on the preparation and catalytic properties for SCR reaction of the iron-oxide pillared/delaminated clay are obtained. This study emphasizes the influence of the preparation conditions on the catalytic activities for the SCR reaction of NO with NH_3.

1. Effects of Different Precursors on SCR Activity

Different salts at different pH values were used in the ion exchange step, and the results are summarized below:

	Pillaring Solution					
Sample	Salt	Aging (hr)	pH	S.A. M^2/g	XRD	Conversion of NO
611	$FeCl_3$	21	1.7	71	-	44%
612	$Fe(NO_3)_3$	21	1.7	150	Amorphous	95.0%
613	$Fe_3Ac_7OH.2H_2]NO_3$	21	3.2	137	Amorphous	73.0%

*All samples were prepared from pillaring solutions formed by hydrolysis of Fe^{3+} salt solutions (0.2M) at the room temperature, using Na_2CO_3 as the base for pH adjustment. The solution/clay ratio was 60 mmol Fe^{3+}/g bentonite.

*The BET N_2 surface areas were measured after outgassing for 1 hr at 200°C in He.

*All samples tested in SCR reaction were precalcined at 400°C in air.

*SCR conditions: NO = NH_3 = 1,000 ppm, O2 = 2%-4%, N_2 = balance, total flow rate = 500 ml/min., catalyst weight = 0.4 g, temperature = 350°C.

It is clear that the nitrate precursor yields the best catalyst.

2. Effects of pH of the Pillaring Solution on the SCR Activity

The effects of the pH value in the ion exchange step on the SCR activity of the final PILC are summarized below. Only the pH value was varied. The SCR activity was tested at 350°C.

Ion Exchange Condition

Sample	pH	Aging (h)	Reaction (h)	NO conversion
621	1.40	16	6	70.5%
622	1.70	16	6	88.5%
623	1.80	16	6	64.0%

*All samples are prepared as follows:

Add a slurry containing 1.0 g Bentonite and 100 ml distilled water into a 0.2 M 300ml $Fe(NO_3)_3$ solution under constant stirring. Change the pH value of the pillaring solution by adding different amounts of Na_2CO_3.

*All PILC samples were pretreated at 400°C (in air) before SCR reaction.

The results above show that the SCR activity is sensitive to the pH value, and that pH = 1.7 yields the best catalyst.

3. Effects of Concentration of the Pillaring Solution on SCR Activity

In this series of experiments, we used $Fe(NO_3)_3$ as the precursor, and fixed pH at 1.7 (as they were the optimal values from B-1 and B-2), and only changed the concentration. The results are summarized below. (The SCR conditions were the same as in B-1.)

Pillaring Conditions

Sample	$Fe(NO_3)_3$ (M)	mmol Fe^{3+}/g bentonite	S.A. (m^2/g)	NO Conversion
631	0.4	120	148	84.0%
632	0.2	60	167	96.0%
633	0.1	30	132	88.2%

All samples were prepared from pillaring solutions formed by hydrolysis of $Fe(NO_3)_3.9H_2O$ at room temperature, using Na_2CO_3 as the base, pH = 1.70. Pillaring time = 96 h. The optimum conditions were those for sample No. 632.

4. Effect of Clay Type on PILC

The bentonite sample used for the synthesis of PILC was a purified form of the natural clay (supplied by Fisher). A commercially available clay was obtained from Laporte, Inc. (Kindly donated by Dr. Gordon Patterson, Laporte Labs,Gonzales,TX). This clay was a synthetic type with well defined structure and properties, with the trade name of Laponite. The chemical structure of Laponite is similar to bentonite. However, the crystal diameter;thickness aspect ratio of Laponite is smaller than bentonite. As a result, it is easier toform delaminated PILC from Laponite. In this work, we use Laponite as the starting clay and compared the resulting PILC with that from bentonite.

Trinuclear acetato hydroxy-iron (III) nitrate, $[Fe_3(OCO\ CH_3)_7OH.2H_2O]NO_3$, was used as the iron cation precursor. It was prepared following the procedure described by Yamanaka et

al. (5). 80.8g $Fe(NO_3)_3.9H_2O$ was dissolved in 50 ml of ethyl alcohol and was subsequently reacted with 140 ml of anhydrous acetic acid. The solution was then cooled in an ice bath. The resulting precipitate was separated and used in the pillaring procedure.

A 0.04 mol/l aqueous solution of the trinuclear acetato hydroxy-iron (III) nitrate was added to a 1% Laponite aqueous slurry under constant stirring. The concentration ratio of themixture was 3.0 mmol iron per gram of Laponite. The mixture was at pH = 3.2 after reacting for 4 h at 35°C. The resulting material was separated by centrifuge and was washed with distilled water 3 times to remove the excess iron ions. It was then dried in air at the room temperature and calcined at 350°C for 6 h.

TheXRD pattern showed no peaks, as shown in Figure 7. The BET N_2 surface area was 243 m^2/g. The NO conversion for SCR was 71% 350°C. The SCR condition was the same as above. It is clear that Laponite (under these conditions) was not as good as bentonite.

Task 8. Promoting Effect of Cr_2O_3 on SCR Activity

The results are shown in Figure 10. A strong promoting effect at 300°C (by doping 2.5% Cr2O3 in the delaminated PILC) was seen. However, a negative effect was seen at higher temperatures. Further studies are under way on promoters for SCR.

Task 9. Effects of significant variable parameters on SCR activities

1. Effects of O_2 on NO Conversion

The effects of oxygen concentration on the SCR of NO with NH_3 over Fe-Bentonite pillared clay catalyst (Sample No. 905) were investigated at atmospheric pressure and 250°-400°C in a quartz fixed bed reactor. The typical experimental conditions were as follows: 0.49 of No. 905 Fe-Bentonite, space velocity = 75,000 h^{-1}, $[NH_3]$ = 1,000 ppm, [NO] = 1,000 ppm, $[O_2]$ = 0%- 4-0%. The reaction was carried out both in the presence and in the absence of oxygen. The results are presented in Figure 11.

Firstly, the results showed that the NO conversion was higher in the presence of oxygen than that in the absence of oxygen. Without O_2 the maximum NO conversion reached 61.0% at 400°C; while 89.5% NO conversion was obtained by addition of 4.0% O_2 to the reactant feed. This result is qualitatively similar to that with the V_2O_5 catalyst where the effect of O_2 is to oxidize the surface V-OH group into V = O group [17, 18].

It was also noted that without oxygen, the NO conversion increased continuously as the reaction temperature increased from 250°C to 400°C.

Task 10. Poisoning Effects of Na_2O. K_2O and Cs_2O on SCR by Fe_2O_3 Pillared Clay

The poisoning effects of Na_2O, K_2O and Cs_2O on Fe-Bentonite catalyst for SCR of NO with NH_3 were studied at 250° - 400°C in a quartz fixed bed reactor. The typical experiment conditions were as follows: 0.40 g catalyst, space velocity = 75,000 h^{-1}, [NH_3] = 1,000 ppm, [NO] = 1,000 ppm and [O_2] = 0% - 4-0%.

The Fe-Bentonite PILC catalysts doped with alkali oxides were prepared by impregnation via incipient wetness with precursor acetate solutions. The impregnated catalysts were dried at 120°C for 12 h and then calcined to decompose the precursor salts. The calcination was carried out at 400°C for 3 h. The amount of metal oxide dopant was 2% by wt. of catalyst for all alkali oxides.

The catalyst activity was measured in terms of % conversion of NO to N_2. Figure 14 shows NO conversion as a function of reaction temperature for the Fe-Bentonite pillared clay catalyst doped with various alkali metal oxides. The results showed that the catalyst activity decreased with both Na_2O and K_2O at all temperatures between 250° and 400°C. The Cs_2O dopant also decreased the NO conversion at reaction temperatures below 350°C. However, when the reaction temperature reached 400°C, the NO conversion actually increased to 85% compared to 78% without the addition of Cs_2O. It seemed that the very strong electron donating ability of cesium played a role in the SCR activity. A redox mechanism might be functional in NO

reduction of the Fe-Bentonite pillared clay catalyst. The addition of cesium may have accelerated the redox process on the catalyst surface. This result is different from that with the V_2O_5/TiO_2 catalyst for SCR of NO with NH_3 [23]. For the V_2O_5 catalyst, all alkalies showed poison effect with Cs being the strongest poison at all temperatures. This difference indicates different mechanisms for the Fe-Bentonite pillared clay and V_2O_5/TiO_2, particularly at higher temperatures (above 350°C). At higher temperatures (350° - 400°C), the very active Cs_2O (resulting from its strong electron donating ability) migrated and dispersed better, which led to a change on the surface. This change promoted the adsorption and reaction of NH_3 and/or NO on the catalyst surface, hence the SCR activity.

Task 11. Effects of SO_2 and H_2O on Ce-Promoted Fe-PILC

Many NO_X containing streams also contain sulfur oxides (SO_X) which can affect the performance of the SCR catalyst [24]. The effect of SO_2 on the SCR reaction is a complex one due to the homogeneous reactions forming ammonium bisulfate [25] and sulfate [26] which deposit on the catalyst surface and block the micropores. On the contrary, reports of promoting effects by SO_2 on SCR activity have been published [23, 27].

As reported in our earlier Quarterly Reports, SO_2 is a poison to the Fe-Bentonite pillared clay catalyst. We also reported that Ce was a strong promoter for the SCR activity of the Fe pillared clay catalyst. Figure 15 shows the effects of sulfur dioxide and water vapor on the catalytic activity of 2% Ce oxide doped Fe_2O_3-pillared clay (Ce-Fe-Bentonite). The reaction conditions were the same as described in Task 1 results. The SO_2 concentration was 1,000 ppm and the H_2O concentration was 5%. The NO conversion decreased slightly when 1,000 ppm SO_2 was introduced into the reactant stream at 400°C Without SO_2, NO conversion was 93% at 350°C, while the NO conversion dropped only slightly to 90% upon the addition of 1,000 ppm SO_2. Furthermore, the effects of adding 1,000 ppm SO_2 and 5% H_2O simultaneously into the reactant stream are also depicted in Figure 2. The results showed only slight decreases in NO conversion upon adding 1,000 ppm SO_2 and 5% H_2O at 350° - 400°C. For example at 350°C,

NO conversion decreased only from 90% to 86%. These results suggest that the FE-Bentonite pillared clay doped with cerium oxide is an effective SCR catalyst that is resistant to sulfur dioxide and water vapor at the practical temperature range of 350° - 400°C.

Task 12. Characterization of the High Activity, Delaminated Fe_2O_3-PILC Catalyst

The detail synthesis procedure and the SCR activity of the delaminated PILC catalyst were reported in an earlier Quarterly Progress Report. A complete characterization was performed and the results are given below.

A1. Mossbauer Spectroscopic Analysis

Transmission Mossbauer spectra were measured using a constant acceleration mode Mossbauer spectrometer with ^{57}Co source at room temperature. The catalyst pellets were ground into a powder and was dispersed and mounted on scotch tape to provide a sample diameter of 25 mm. Spectra are reported relative to iron foil.

The Mossbauer spectra are shown in Figure 16. Upon examination of Fig. 16, it is apparent that there are contributions from a center doublet, surrounded by a sextuplet. First, the outside six peaks can be fit as a sextuplet. The two peaks in the center are fit as an equal area doublet. The parameters from this initial fit are shown in Tables 3 and 4. Table 3 contains the sextuplet parameters and Table 4 contains the doublet parameters.

The literature on Mössbauer spectra of iron oxide pillared clays (28-32) show only a doublet, even though bulk iron oxides such as Fe_2O_3 and Fe_3O_4, exhibit magnetic hyperfine splitting, giving six lines instead of two. This is the result of superparamagnetism; essentially the particles are too small to exhibit hyperfine splitting.

Now we discuss the magnetic components of the spectrum. First, similar systems yielding spectra similar to Fig. 16 are observed in the literature (33-35). There are differing values reported for similar systems shown in Table 3, and the variations are due to differences in particle size. For particles in a narrow size range, about 100-600Å, an average particle size can

be estimated from the value of the hyperfine field. For the bulk Fe_2O_3, the accepted value is around 515-518 kOe. As the particle size is reduced below 600 Å, the value of hyperfine field gets smaller until the magnetically split component collapses into a doublet at about 130 Å, due to superparamagnetism (36). Using only the data in Table 3, it is apparent that a value of the particle size in the delaminated clays is about 170 Å. This result is consistent with that from XRD line broadening reported in a previous Quarterly Progress Report.

A correlation between the average particle volume and the percent superparamagnetic contribution has been done for α-Fe_2O_3 (25). The percent superparamagnetic in the case of Fig. 16 is 31.6%. There are 3 components of the delaminated PILC that contribute to this doublet: (1) the 3 wt % Fe_2O_3 impurity in the bentonite clay, (2) iron pillars, and (3) the superparamagnetic contribution from 170 Å particles. Using the previously mentioned correlation, 170 Å particles will give a 10% doublet contribution. Subtracting the contribution of the bulk particles leaves an estimated 22% Fe_2O_3 contribution from the iron pillars and 3% iron wt % clay impurity. This 3% wt % clay impurity is about 7% of the Fe_2O_3 is the sample, leaving about 15% of the iron in pillared form.

To maximize the resolution of the central two doublets, another Mossbauer spectrum was taken by adjusting the velocity range to +/- 4 mm/sec from +/- 10 mm/sec and recalibrating the mössbauer with sodium nitroprusside. In this case, the data from the sextuplet in Fig. 16 was entered as an invariant into the mössbauer fitting procedure. Thus, only the fitting of the equal area doublet was carried out. Results from this fitting yielded no significant improvements of the doublet fit. Table 5 contains a comparison of the doublet parameters with published iron pillared clay mössbauer results. The literature data on pillared clays are devoid of hyperfine splitting. The large variations in parameters are clearly seen in Table 5. Although it is known (28-32) that the major contribution to Doublet II is from iron oxide pillars, iron impurities in the clay also make a contribution.

Summarizing the Mossbauer characterization results, the structure of the delaminated sample can be described as "house-of-cards," and a schematic representation of the structure is

shown in Fig. 17. This picture is also consistent with our XRD results reported in the Quarterly Progress Report, as well as the micropore probing results to be given below.

A2. Micropore Size Distribution by Molecular Probing

The existence of micropores and the micropore size distribution in the delaminated clay sample were further studied by sorption of probe molecules at subcritical temperatures. Under subcritical conditions, micropore filling takes place and the micropore volumes can be calculated.

Thermogravimetric analysis (TGA) was employed to measure the weight gains, by sorption of molecules with known dimensions. Pore volumes for different pore dimensions were measured in this manner.

Three probe molecules were used, with their kinetic diameters given below: N_2 (3.6 Å), n-hexane (4.9 Å) and 1,3,5 trimethyl benzene (8.6 Å). The cumulative pore volumes were calculated from the equilibrium sorption amount assuming the adsorbate as liquid. The equilibrium sorption amounts of n-hexane and trimethyl benzene were measured at room temperature by TGA. The N_2 sorption was measured at 77K with the Quantasorb Analyzer. The results are shown in Fig. 18. For the N_2 sorption, the αs method was used to obtain the micropore volume (37). From the data shown in Fig. 18, it is seen that a significant amount of micropores with dimensions smaller than 9 Å existed in the delaminated sample. For the Fe_2O_3 pillared clay, the cumulative pore volume by N_2 sorption was 0.19 cm^3/g, compared to 0.13 cm^3g for the delaminated clay. From this result, it is clear that the delaminated sample contained pillared clay fragments, thus it should be properly referred to as delaminated pillared clay.

A3. In Situ FT-IR Characterization

To examine the surface acidity and to identify the Brønsted and Lewis acid sites of the delaminated/pillared clay, FT-IR spectra of adsorbed ammonia were measured. The IR spectra

were measured with a Nicolet Impact 400 FT-IR spectrometer. The samples were pressed into self-supporting disks. The typical weight of the prepared disks was 60-70 mg, which was equivalent to 12-14 mg/cm^2. The *in situ* IR spectra of NH_3 adsorbed on pillared/delaminated clays were recorded by using an IR cell that allowed the sample to be treated at high temperatures under vacuum or in different gases. The samples were pretreated at 300°C in vacuo for 2 hours prior to adsorption. The spectra of adsorbed ammonia at room temperature are shown in Fig. 19.

Figure 19 shows the effects of water vapor on the absorption bands at 1636.7, 1458, and 1595.1 cm^{-1}. The peak at 1636.7 cm^{-1} is attributed to the bending vibration of surface hydroxyl groups (38). The negative absorption band in spectra (a) and (b) were due to the consumption of surface hydroxvl groups by ammonia adsorption, since all spectra were ratioed against that of the sample before NH_3 exposure. Similar negative peaks were also observed when ammonia was adsorbed on V_2O_5/SiO_2 (39). The strong peak at 1458 cm^{-1} was due to ammonia adsorbed on Brønsted acid sites (40). The weak peak at 1595.1 cm^{-1} was likely due to ammonia coordinatively adsorbed on the catalyst surface, i.e., on Lewis acid sites.

Figure 19 shows that the IR band at 1637 cm^{-1} changed from a negative one to a position one, after about 3 minutes of exposure to 2% H_2O. It is interesting to note that the peak intensity at 1458 cm^{-1} actually increased in the first few minutes upon H_2O exposure. Concurrently, the weak band at 1595 cm^{-1} gradually decreased and eventually disappeared. This suggests that,with the addition of water vapor, the Lewis acid sites were converted to Brønsted acid sites and the coordinatively adsorbed ammonia was transformed into ammonium ions on the surface.

For clays and their variants, the surface acidity and the type of acid sites (Brønsted or Lewis sites) are dependent on the extent of hydration-dehydration. The FT-IR spectrum of ammonia adsorbed on the delaminated/pillared clay at 150°C is shown in Fig. 20. A very strong and sharp peak at 1453 cm^{-1} was observed. The difference with the spectra taken at room temperature was that there was no negative band at around 1630 cm^{-1}. This was due to dehydration at 150°C which eliminated the adsorbed water molecules.

The IR results showed that the delaminated/pillared clay was abundant in Brønsted acid sites on the surface. As shown in our previous work (41-43) Brønsted acid sites on V_2O_5 and other oxides are the active sites for selective catalytic reduction of NH_3 with NO. The high catalytic activity for SCR of this clay catalyst may be correlated with its strong Brønsted acidity.

Figure 21 shows the IR spectra of ammonia adsorbed on montmorillonite and the delaminated/pillared clay on the same intensity scale. Ammonia adsorbed on montmorillonite also gave an absorption band at around 1450 cm^{-1}, but its relative intensity was low. It is known that there are only Lewis acid sites on Fe_2O_3 (44, 45). The origin of the strong Brønsted acid sites in this clay catalyst was probably the result of the interactions between Fe_2O_3 and the clay. Furher studies of these interactions are in progress.

Task 13. Mechanism of SCR of NO by NH_3 on Pillared Clay Catalyst: Temperature Programed Desorption (TPD) Studies

We have used TPD techniques during the past three months to study the mechanism of the SCR reaction on the pillared clay catalyst. Before our studies, TPD results on the vanadia type catalyst in the literature showed that NH_3 chemisorbs strongly at the reaction temperatures (i.e., above 300°C), whereas NO does not. For the pillared clay catalyst, NH_3 also chemisorbs strongly at the reaction temperatures. Therefore, NO chemisorption would provide key information on the understanding of the SCR reaction on this catalyst.

Temperature programmed desorption (TPD) of NO_X on pillared clay was carried out in the same apparatus as that used for measuring the kinetic data of the SCR reaction, which was reported in detail in earlier reports. Before NO was adsorbed on the catalyst surfaces, the catalysts were heated to 400°C in N_2 and were kept at this temperature for 2 hrs. As stated in the following text, some of the TPD experiments were conducted after the catalysts were subjected to the SCR reaction for a given time. In all of the TPD experiments, the heating rate was kept at 10°C/min and the sample amount was 0.4 g. Nitrogen gas was used as the purge/carrier gas, at 350 ccSTP/min. Before measurement for the TPD signal, the gas phase NO was purged by N_2

until the base line reached a steady state. The concentrations of NO or NO_2 were monitored by the chemiluminescent NO/NO_X analyzer. Both clay and pillared clay were included in our TPD studies.

The TPD characteristics were significantly different for NO chemisorbed on the montmorillonite clay and that on the Fe_2O_3-pillared clay, so they will be discussed separately.

The first observation was that the chemisorpdon of NO was substantially enhanced in the presence of O_2, for both montmorillonite clay and the Fe_2O_3 pillared clay. Figure 22 shows the TPD profile of NO adsorbed on the clay (in the absence of O_2). The equivalent TPD profile for NO adsorbed in the presence of 2% O_2 is showed in Figure 23. The amount of NO chemisorbed on the clay was increased by the presence of O_2 by approximately a factor of 7-8. Although the amounts were vastly different, the TPD peak positions were essentially the same. The peak desorption temperatures for NO chemisorbed in the absence of O_2 were: 75,330 and 600°C, and that in the presence of O_2 were: 61,340 and 600°C.

The TPD profile for NO (chemisorbed in the presence of O_2) from the delaminated Fe_2O_3-pillared clay is shown in Figure 24. A major difference between the TPD profiles from the clay and the pillared clay was apparent. The large peak at 330°-340°C for the clay sample was substantially reduced and shifted toward a lower temperature (225°C), while the large peak at 75°C and the small peak at 600°C remained. For the Fe_2O_3-PILC TPD, a large amount of $N0_2$ was desorbed.

In order to obtain insight into the relationship between the TPD characteristics and thc SCR activity, a series of NO TPD experiments were performed after the SCR reaction or NO adsorption both at 400°C. The PILC catalyst was heated to 400°C and was kept at this temperature for 30 minutes. A gas containing 1,000 ppm NO and 2% O_2 in N_2 was passed through the catalyst bed for 30 minutes. After the gas phase NO was purged by N_2 for 30 minutes, 1,000 ppm NH_3 was passed through the catalyst bed to react with the adsorbed NO for 20 minutes. Before heating to 650°C, the catalyst was purged in N_2. The TPD profiles from these experiments were different from those in the previous ones. There were two peaks in these

TPD profiles, one at about 420°C, the other at near 650°C. The temperature ramp between 400°C and 650°C was repeated after the first TPD run, without further NO or NH_3 treatments. Desolption of NO_X continued at the same peak temperatures during the ensuing ramps, with gradually decreasing peak intensities. Figure 25 shows the results from the first TPD ramp and the third ramp. The same results were obtained when TPD measurements were made after the PILC catalyst was subjected to the SCR reaction at 400°C. This result indicated that the adsorbed species corresponding to TPD peaks at 420°C and 650°C were not active species for the SCR reaction, and that the NO was very strongly bonded to the pillard clay catalyst. Bonding of the NO_X molecules within the clay lattice was a possibility.

As mentioned, NO does not chemisorb on V_2O_5 at temperatures above 300°C, and this was the basis for the Eley-Rideal type mechanism proposed for the NO SCR reaction with NH_3 (see, e.g., 46, 1992; 47, 1995). From the TPD results for the Fe_2O_3-PILC catalyst, it is seen that a significant amount of NO_X is chemisorbed at temperatures up to 600°C, i.e., well above the SCR reaction temperature of 350°-400°C. It is, therefore, reasonable to conclude that SCR reaction on the Fe_2O_3-PILC follows a different type of mechanism, i.e., that of the Langmuir-Hinshelwood type, involving both chemisorbed NO_X and NH_3 (or NH_X).

Task 14. SCR by Fe Ion-Exchanged TiO_2-Pillared Clay

As reported in the last quarterly report, pore diffusion resistance has a strong influence on SCR of NO with NH_3 over the Fe-Bentonite pillared clay catalyst. In order to minimize the pore diffusion limitation, we tried to increase the pore dimensions of the catalysts. It is known that TiO_2-pillared clay has a stable structure and also has larger pores. Consequently, our approach was to use TiO_2 PILC and do ion exchange with Fe^{+3} to replace the H^+ on the PILC. (Ion exchange should not decrease the pore dimensions appreciably.) Thus, TiO_2-PILC was ion exchanged with an $Fe(NO_3)_3$ solution. The ion-exchanged product was tested for SCR of NO with NH_3.

A. Preparation of Fe-Ti-PILC

Titania pillared clay (TiO_2-PILC) was first prepared following the procedure suggested by Sterte (48). The following staring materials were used: a purified montmorillonite, a purified-grade bentonite powder from Fisher Co. (with particle sizes less than or equal to 2 - μm) and titanium chloride ($TiCl_4$) (also from Fisher) was used as the pillaring precursor. A 5-gram sample of montmorillonite was dispersed in 0.5 l of distilled water by prolonged stirring. The amount of pillaring agent required to obtain a Ti/clay ratio of 10 (mmol of Ti)/(g of clay) was then added to the vigorously stirred suspension. The resulting product was separated by vacuum filtration and washed with distilled water several times until the liquid phase was free of chloride ions as determined by titration with $AgNO_3$. The final product was dried in air for 10 h, followed by calcination at 400°C for 3 h.

The above TiO_2-PILC was ion-exchanged with iron nitrate aqueous solution by using a conventional ion exchange procedure (49). One g of TiO_2-PILC was added to 100 ml water containing 2 x 10^{-2} mol/l iron nitrate. The mixture was stirred for 24 h at room temperature. The solid was removed by filtration and washed several times, and the above ion exchange procedure was repeated 5 times. The final product was dried at 120°C and calcined at 400°C.

B. NH_3 SCR Activities Over Fe-Ti-PILC

The SCR reaction was carried out in a fixed bed reactor over the iron ion-exchanged TiO_2-PILC (Fe-Ti-PILC). The reaction conditions were as follows: [NO] = 1,000 ppm, [NH_3] = 1,000 ppm, [O_2] = 3%, N_2 = balance, totral flowrate = 500 cm^3/min. and catalyst weight = 0.4 g.

Fig. 26 shows the SCR activities of Fe-Ti-PILC with and without 1,000 ppm SO_2 and 5% water vapor in the reactant stream. A commercial SCR catalyst, WO_3 + V_2O_5/TiO_2, was also tested as the standard for comparison, also shown in Figure 3. For Fe-Ti-PILC catalyst, without SO_2 and water vapor, the maximum NO conversion was 72% at 500°C. However, in the presence of SO_2 and H_2O, it reached about 98%. Moreover, it remained high between a wide

temperature range, 450° to 550°C. On the other hand, for the WO_3 + V_2O_5/TiO_2 catalyst, the NO conversion remained high (that is, 97%) at temperatures below 400°C without water vapor and sulfur dioxide. With the addition of SO_2 and H_2O, the SCR activity decreased slightly at 400°C but substantially at 300°C and 350°C.

The effects of SO_2 and H_2O are negative for all known SCR catalysts. The strong positive effects shown in Figure 3 are unexpected but welcome. The reason for this positive effect is not understood.

The results shown in Fig. 3 indicate that the iron ion-exchanged TiO_2-PILC is an excellent SCR catalyst for high temperature applications. Applications for internal combustion engines require the temperature range 500° - 550°C, and mordenite-type catalysts (e.g. Zeolon) are being used for these applications.

Task 15. SCR by Fe_2O_3/TiO_2 Catalyst

Fe_2O_3 is known to be an active catalyst for SCR of NO with NH_3 [50, 51]. In particular, Fe_2O_3 pillared/delaminated clay is a very active catalyst for SCR of NO with ammonia [51]. However, intracrystalline diffusion limitation was very strong over the Fe_2O_3 pillared/delaminated clay catalyst for SCR of NO with ammonia as reported in the last quarterly report.

In order to minimize the diffusion resistance limitation as well as using the active component of Fe_2O_3 for the SCR of NO with ammonia, we explored another possible support with large pore dimensions through the sol-gel route to eliminate the diffusion limitation. The active catalytic component, Fe_2O_3, was supported on the sol-gel support, and its catalytic activity on the SCR of NO was tested.

It is well known that some oxides with high specific surface areas and pore volumes can be obtained by sol-gel processes [52, 53]. While there are numerous reports concerning the SCR of NO over supported TiO_2, particularly V_2O_5/TiO_2 [54]. Studies of the SCR of NO over catalysts prepared by the sol-gel process are rare except by Baiker et al. [55] and Ko et al. [56].

We first prepared a porous TiO_2 support by the sol-gel process, and supported Fe_2O_3 on this TiO_2 carrier. The Fe_2O_3 supported on TiO_2 (Fe_2O_3/TiO_2) was used as the catalyst for SCR of NO with ammonia. The experiments and results are as follows:

A. Preparation of TiO_2 Support by the Sol-Gel Process

The TiO_2 sample was prepared by adding dropwise 0.2 M HNO_3 solution to the titanium tetrabutanoxide ($Ti(OBu)_4$) diluted in CH_3OH under vigorous stirring. The concentration was adjusted carefully to yield the final molar ratio $TI(OBu)_4:H_2O:CH_3OH = 1:5:100$. The process was facilitated with HNO_3 as the catalyst. After the sol changed into gel, the sample was washed repeatedly with distilled water and covered with distilled water for aging that lasted for 24 hrs. The sample was finally dried and calcined at 400°C. The specific surface area of the resulting sample was measured by the BET method to be 120 m^2/g. This value was very high as compared with the value of 25 m^2/g for the commercial Degussa TiO_2.

B. SCR by Fe_2O_3 Supported on Sol-Gel TiO_2 Catalyst

The above TiO_2 sample was impregnated in the iron nitrate aqueous solution by the incipient wetness method. After the sample was dried and calcined at 400°C, the SCR activities of NO with ammonia were tested in a quartz fixed bed reactor as described earlier. The typical reaction condtions were as follows: [NO] = 1,000 ppm, $[NH_3]$ = 1,000 ppm, O_2 = 2%, N_2 = balance, total flowrate = 500 ml/min. catalyst weight = 0.40 g. The SCR activity as a function of temperature is shown in the following table.

SCR Activity by Fe_2O_3/TiO_2 (Sol-Gel) Catalyst

NO Conversion (%)

T,°C	250	300	350	400
without SO_2	2	50	71	40
with SO_2	-	48	70	-

Task 16. SCR by C_2H_4

EXPERIMENTAL

TiO_2-pillared clay was prepared following the procedure of Sterte (57) The starting material was a purified montmorillonite (bentonite) powder from Fisher, with crystal sizes less than or equal to 2μm. Titanium chloride ($TiC1_4$), also from Fisher, was used as the TiO_2 precursor. After pillaring (57), the resulting PILC was separated by vacuum filtration, and washed with distilled water until the filtrate water was free of chloride ions as determined by titration with $AgNO_3$. The PILC was then dried at 120°C for 10 h, and calcined at 400°C in air for 3 h.

The TiO_2-PILC was ion exchanged with copper nitrate solution following the conventional ion-exchange procedure. Copper nitrate was used as the source of Cu^{2+} ions. One g of TiO_2-PILC was added to 100 ml of 0.02 M copper nitrate aqueous solution. The mixture was stirred for 24 h at 70°C. The pH of the starting solution was adjusted to pH = 6.0 by adding proper amounts of ammonia solution. The ion-exchanged product was collected by filtration followed by washing with distilled water 5 times. This ion exhange procedure was repeated 3 times. Then the product was dried at 120°C followed by calcination at 400°C in air.

The SCR activity was measured with the same reactor system described elsewhere, and the same experimental details were followed (58). That the measured conversion was NO_X reduction to N_2 was confirmed by the NO_X mode of chemiluminescent analyzer and mass spectrometric analysis for N_2.

RESULTS AND DISCUSSION

The SCR activities of the Cu^{2+} ion exchanged TiO_2 pillared clay have been measured at five temperatures: 200, 250, 300, 350, and 400 degrees C. C_2H_4 was used as the reducing gas. Also, Ce_2O_3 was tested as a promoter. The effects of SO_2 and H_2O have also been tested. The experimental conditions were chosen to be the same as that reported in the literature for the Cu-

ZSM-5 catalyst (59,60), so a direct comparison could be made. The reaction conditions were as follows: NO = 1,000 ppm, O_2 = 2%, C_2H_4 = 250 ppm, N_2 = balance, total flowrate = 150 ml/min. and catalyst weight = 0.5 g.

The activities for SCR of NO by ethylene over Cu^{2+}-exchanged TiO_2-PILC are shown in Fig. 27. The results reported by Iwamoto et al. on Cu-ZSM-5 (60, 59) are also shown in Fig. 1, for a direct comparison. Estimates of rate constants may be made from the conversion data based on two assumptions: the reaction is first-order (with respect to NO), and it is without diffusion limitation (which is not the case). The following rate constants (k) can thus be obtained following the integral analysis that we adopted previously (28): At 250°C: k (in $cm^3/g/s$) = 9.72 (A), 5.57 (B) and 4.47 (C); At 300°C: k = 14.56 (A), 10.09 (B) and 3.58 (C). Here A refers to Cu^{2+} exchanged PILC without $S0_2$, B refers to that with $S0_2$ and H_20, and C refers to Cu^{2+}-ZSM-5 without SO_2 and H_2O.

Figure 27 shows that the catalytic activity increased with increasing temperature, reaching a maximum of 79% NO conversion at 300°C, and then decreased at higher temperatures. It is clear that the Cu^{2+} exchanged TiO_2-PILC is substantially more active than the Cu-ZSM-5 catalyst. In the presence of H_2O (5%) and SO_2 (500 ppm), the activities of Cu^{2+}-exchanged TiO_2-PILC decreased, as expected. However, these decreased activities were still higher than that of Cu-ZSM-5 under SO_2/H_20-free conditions (Fig. 27).

Cerium is known to be a promoter for SCR by NH_3 (26). Ce_2O_3 (0.5% wt.) was doped into the Cu^{2+}-TiO_2-PILC catalyst by incipient wetness impregnation using Ce(III) nitrate hexahydrate solution. The impregnated sample was calcined in air at 400°C. Obviously, Ce(IV) was formed upon calcination and also during the reaction. The C_2H_4 SCR activities of the Ce doped catalyst are shown in Fig. 28. The ceria dopant increased the C_2H_4 SCR activity at tempertures higher than 300°C, but decreased the activity at 250°C. The reason for the decrease is not known, although it could be related to poor dispersion (or sintering) of ceria at this temperature. The effect of SO_2 + H_2O on the activity of the Ce-doped catalyst is also shown in Fig 28, where a decrease but a still high activity was seen. The catalytic activities were fully

recovered after SO_2 and H_2O were switched off. Thus, SO_2/H_2O did not alter (or poison) the active sites; rather, they probably occupied the sites reversibly.

A catalyst stability test was performed for the Ce-doped catalyst at 300°C in the presence of both SO_2 and H_2O. A decrease of approximately 3% in NO conversion was observed upon a 48-hour run. Further and more definitive experiments are underway. However, it is clear that this catalyst is far more stable than Cu-ZMS-5.

The higher activities of the Cu^{2+} exchanged pillared clay than the Cu^{2+} exchanged ZSM-5 can be attributed to at least two reasons. Firstly, the cation exchange capacities (CEC) of pillared clays are considerably higher than that of ZSM-5. A typical CEC value for pillared clays is 1 meq/g, which is about twice that of the ZSM-5 with a low Si/Al ratio (of 20). Secondly, the pore dimensions in the pillared clays are considerably larger than that in ZSM-5, and pore diffusion resistance is significant in the SCR reaction (61, 62). The pore size distributions in pillared clays are typically in the range 5 - 15Å (63, 64), compared to the channel dimensions of the order of 5Å in ZSM-5. Moreover, it is possible that there exists a more favorable chemical environment (for redox) for the Cu^{2+} ion in the pillared clay than in the structure of zeolite, and this may also be the reason for the H_2O resistance of the pillared clay catalyst. The residual Brönsted acidity also helps activate the hydrocarbon for the reaction (65).

REFERENCES

1. Klug, H.P., and Alexander, L.E., "X-Ray Diffraction Procedures -- For Polycrystalline and Amorphous," 2nd Ed., Wiley, New York, Chapt. 9, (1974).
2. Ibid, p. 667.
3. Bailey, S.W., "Structures of Clay Minerals and Their X-Ray Identification," Ed. by G.W. Brindley and G. Brown, Mineralogical Society Monograph, No. 5, Mineralogical Society, London, 1980.
4. Mott, C.J.B., "Clay Minerals - An Introduction," in "Pillared Clays," Ed. by R. Burch,*Catalysis Today*, **2**, 187 (1988).
5. Burch, R., and Warburton, C.I., *J. Chem. Soc. Chem. Commun.* **117**, (1987).
6. Figueras, F., *Catal. Rev. Sci. Eng.*, **30**, 457 (1988).
7. Pinnavaia, T.J., Tzou, M-S., Landau, S.D., Raythatha, R., *J. Mol. Catal.*, **27**, 195 (1984).
8. Occelli, M.L., Landau, S.D., and Pannavaia, T.J., *J. Catal.*, **90**, 256 (1984).
9. Occelli, M.L., Landau, S.D., Pinnavaia, T.J., *J. Catal.*, **104**, 331 (1987).
10. Pinnavaia, T.J., Tzou, M.S., and Landau, S.D., Pillared and Delaminated Clays Containing Chromium. U.S. Patent, 4,665,045, May 12, 1987.
11. Occelli, M.L., Landau, S.D., Pinnavaia, T.J., *J Catal.*, **104**, 331 (1987).
12. Reference (1), p. 371 and the literature cited therein.
13. Chen, J.P., and Yang, R.T., *Appl. Catal.*, **80**, 135 (1992).
14. Tuenter, G., Leeuwen, W.F.V., and Snepvangers, L.J.M., *Ind. Eng. Chem. Prod. Res. Dev.*, **25**, 633 (1986).
15. Wong, W.C. and Nobe, K., *Ind. Eng. Chem. Prod. Res. Dev.*, **25**, 179 (1986).
16. Rightor, E.G., Tzou, M.S. and Pinnavaia, T.J., *J. Catal.*, **130**, 29 (1991).
17. Bosch, H. and Janssen, F., *Catal. Todav.*, **2**, 433 (1988).
18. Markvart, M. and Pour, H., *J. Catal.*, **7**, 279 (1967).
19. Willey, J. and Peri, J.B., in *"Microstructure and Properties of Catalyst, "* in M.M.J. Treacy, J.M. Thomas, J.M. White, eds.), p. 359, Material Research Society, Philadelphia, PA (1988).
20. Weiz, P.B. and Prater, C.D., *Adv. Catal.*, **4**, 143 (1954).
21. Shelef, M., Otto, K. and Gandi, H., *Atm. Environ.*, **3**, 107 (1969).
22. Nunan, J.G., Silver, R.G. and Bradley, S.A., in *"Catalytic Control of Air Pollution,"* Chapter 7, R.G. Silver, J.E. Sawyer, J.C. Summers, eds., American Chemical Society, Washington, 1992.
23. Chen, J.P. and Yang, R.T., *J. Catal.*, **125**, 411-420 (1990).
24. Bosch, H. and Janssen, F., *Catal. Today*, **2**, 433 (1988).

25. Matsuda, S., Kamo, T., Kato, A., Nakajima, F., Kumara, T. and Kurada, H., *Ind. Eng.Chem. Prod. Res. Dev.*, **21**, 48 (1982).
26. Yoshida, H. Takahasi, K., Sekiya, Y., Morikawa, S. and Kurita, S., in *"Proceedings of 8th Congress on Catalysis, Berlin, 1988,"* Vol. 3, p. 649.
27. Nam, I., Eldridge, J.W. and Kittrell, J.R., *Ind. Eng. Chem. Prod. Res. Dev.*, **25**, 192 (1986).
28. Doff, D.H., Gangas, N.H.J., Allan, J.E.M. and Coey, J.M.D., *Clay Minerals*, **23**, 367 (1988).
29. Martin-luengo, M.A., Martin-scarvalho, H., Ladriere, J. and Grange, P., *Clay Minerals*, **24**, 495 (1989).
30. Occelli, M.L., Stencel, J.M., and Suib, S.L., *J. Mol. Catal.*, **64**, 221 (1991).
31. Lee, W.Y., Tatarchuk, B J. and Raythatha, R.H., *J. Catal.*, **115**, 159 (1989).
32. Yamanaka, S. and Hattori, M., *"Iron Oxide Pillared Clay,"* in Pillared Clays, ed. R. Burch, *Catalvsis Today,* **2**, 261 (1988).
33. Lund, C.R.F. and Dumesic, J.A., *J. Phvs. Chem.*, **85**, 3175 (1981).
34. Hobson, M.C. and Gager, H.M., *J. Catal.*, **16**, 254 (1970).
35. Kundig, W. and Bommel, H., *Phvs. Rev.*, **142**, 327 (1966).
36. Yoshioka, T., Koezukz, J. and Ikoma, H., *J. Catal.*, **16**, 264 (1970).
37. Gregg, S.J. and Sing, K.S.W., "Adsorption, Surface Area and Porosity," Academic Press, London, 2nd ed., 1982.
38. Little, L.H., "Infrared Spectra of Adsorbed Species," Academic Press, London, 1966.
39. Rajadhyaksha, R.A. and Knozinger, H., *Appl. Catal.*, **51**, 81 (1989).
40. Kung, M.C. and Kung, H.H., *Catal. Rev.Sci. Eng.*, **27**, 425 (1985).
41. Chen, J.P. and Yang, R.T., *J. Catal.*, **125**, 411 (1990).
42. Yang, R.T., Chen, J.P., Kikkinides, E.S., Cheng, L.S. and Cichanowicz, J.E., *Ind. Eng.Chem. Res.*, **31**, 1440 (1992).
43. Chen, J.P. and Yang, R.T., *J. Catal.*, **139**, 277 (1993).
44. Rochester, C.H. and Topham, S.A., *J. Chem. Soc. Faradav Trans. I*, **75**, 1259 (1979).
45. Peri, J.B., *J. Phvs. Chem.*, **69**, 220 (1965).
46. Went, G.T., Leu, L., Rosin, R.R. and Bell, A.T., *J. Catal.*, **134**, 492 (1992).
47. Topsoe, N.Y., Dumesic, J.A. and Topsoe, H., *J Catal.*, **151**, 241 (1995).
48. Sterte, J., *Clays Clay Miner.*, **34**, 658 (1986).
49. Daden, D. and Streat, M., *"Ion Exchange Technology,"* Society of Chemical Industry, London 1984.
50. Niiyama, H., Ookawa, T. and Echigoya, E., *Nippon Kagaku Kaishi.* 1871 (1975).
51. Chen, J.P., Hausladen, M.C., and Yang, R.T., *J. Catal.*, **151**, 135-146 (1995).
52. Brinker, C.J., *Sol-Gel Science*, Harcourt Brace Jovanovich, Boston, 1990.

53. Klein, L.C., Sol-Gel Technology for Thin Films, Fibers, Preforms, Electronics, and Speciality, Shaples, Noyes, Park Ridge, New Jersey (1988).
54. Bosch, H., and Janssen, F., *Catal. Today*, **2**, 369 (1988).
55. Gasser D., and Baiker, A., *J. Catal.*, **113**, 325 (1988).
56. Miller, J. B., Rankin, S. E., and Ko, E. I., *J. Catal.*, **148**, 673 (1994)
57. Sterte, J., *Clays Clay Miner.*, **34**, 658 (1986).
58. Chen, J.P. and Yang, R.T., *J. Catal.*, **125**, 411 (1990).
59a. Shelef, M., *Chem. Rev.*, **95**, 209 (1995).
59b. Sato, S., Yu-u, Y., Yahiro, H., Mizuno, N. and Iwamoto, M. *Appl. Catal.*, **70**, L1 (1991).
60. Iwamoto, M. and Mizuno, N., *Proc. Inst. Mech. Eng. Part D,* J. *Auto. Eng.*, **207**, 23 (1993).
61. Taylor, K.C., in "Catalysis: Science and Technology," (J.R. Anderson and M. Boudart, eds.), Vol. 5, Springer-Verlag, Berlin, 1984.
62. Li, Y. and Armor, J.N., *J. Catal.*, **150**, 376 (1994).
63. Yang, R.T. and Baksh, M.S.A., *AIChE J.*, **37**, 679 (1991).
64. Baksh, M.S.A., Kikkinides, E.S. and Yang, R.T., *Ind. Eng. Chem. Res.*, **31**, 2181 (1992).
65. Chen, J.P. and Yang, R.T., *Appl. Catal.*, **80**, 135 (1992).

Table 1. Chemical Compositions (% by wt.) of Clay and Pillared Clays

	Montmorillonite	Delaminated Fe_2O_3-PILC	Fe_2O_3-PILC
SiO_2	60.32	44.36	59.19
Al_2O_3	19.14	13.93	19.63
Fe_2O_3	3.66	30.61	9.55
TiO_2	0.16	0.15	0.18
CaO	1.41	0.55	0.47
MgO	2.35	1.56	2.06
Na_2O	2.88	0.59	0.65
K_2O	0.51	0.33	0.34
H_2O	8.50	3.54	3.06
Total	98.93	95.61	95.13

Table 2. Longevity Test of SCR Activity for the Delaminated Fe_2O_3 Pillared Clay

Time (Hr)	2*	3	24	48	96	97*
NO Conversion (%)	97.5	84.0	83.0	85.0	84.5	98.8

Reaction conditions: NO = NH_3 = 1,000 ppm, O_2 = 2%, SO_2 = 1,000 ppm (when used), H_2O = 8% (when used), total flowrate = 500 ml/min, catalyst = 0.4 g, 400°C.

*Reaction without water vapor and SO_2.

Table 3. Magnetically Split Component: The Sextuplet

Hyperfine Field (kOe)	Isomer Shift (mm/sec~	Identified Species	Reference
501	0.351	Fe2O3	this work
496	–	158 A particles Fe203/SiO2	7
516	–	650 A particles Fe303/SiO2	7
503	0.38	180 A particles Fe203/SiO2	8
518	0.39	bulk a-Fe203	8

Table 4. Superparamagnetic Component: the Doublet

Isomer Shift (mm/s)	Quadrupole Splitting (mm/s)	% Superpara-magnetic	Identified Species	Reference
0.304	0.738	31.6	Fe2o3	This work
0.328	0.811	63	α–Fe2O3/SiO2	6
0.60	0.68	45	158 A particles Fe203/SiO2	7
0.56	0.71	70	650 A particles Fe203/SiO2	7
0.38	0.44	–	180 A particles Fe203/SiO2	8
–	–	O	bulk α–Fe203	8
0.63	0.73	100	7% wt α–Fe2O3/SiO2	59

Table 5. The Doublets Parameters: Comparison with Iron Pillared Clays

Doublet l: Isomer Shift mm/s	Doublet 1: Quadrupole Splitting mm/s	Doublet l: % Relative Area	Doublet 2: Isomer Shift mm/s	Doublet 2: Quadrupole Splitting mm/s	Doublet 2: % Relative Area	Reference
–	–	–	.304	.738	31.6	This work
0.30	1.29	29	0.33	0.74	68	
0.33	0.93	49	0.34	0.54	51	2
0.34	1.14	62	0.35	0.70	38	3
–	–	–	0.37	0.76	100	4
0.42	1.41	17	0.38	0.72	83	5

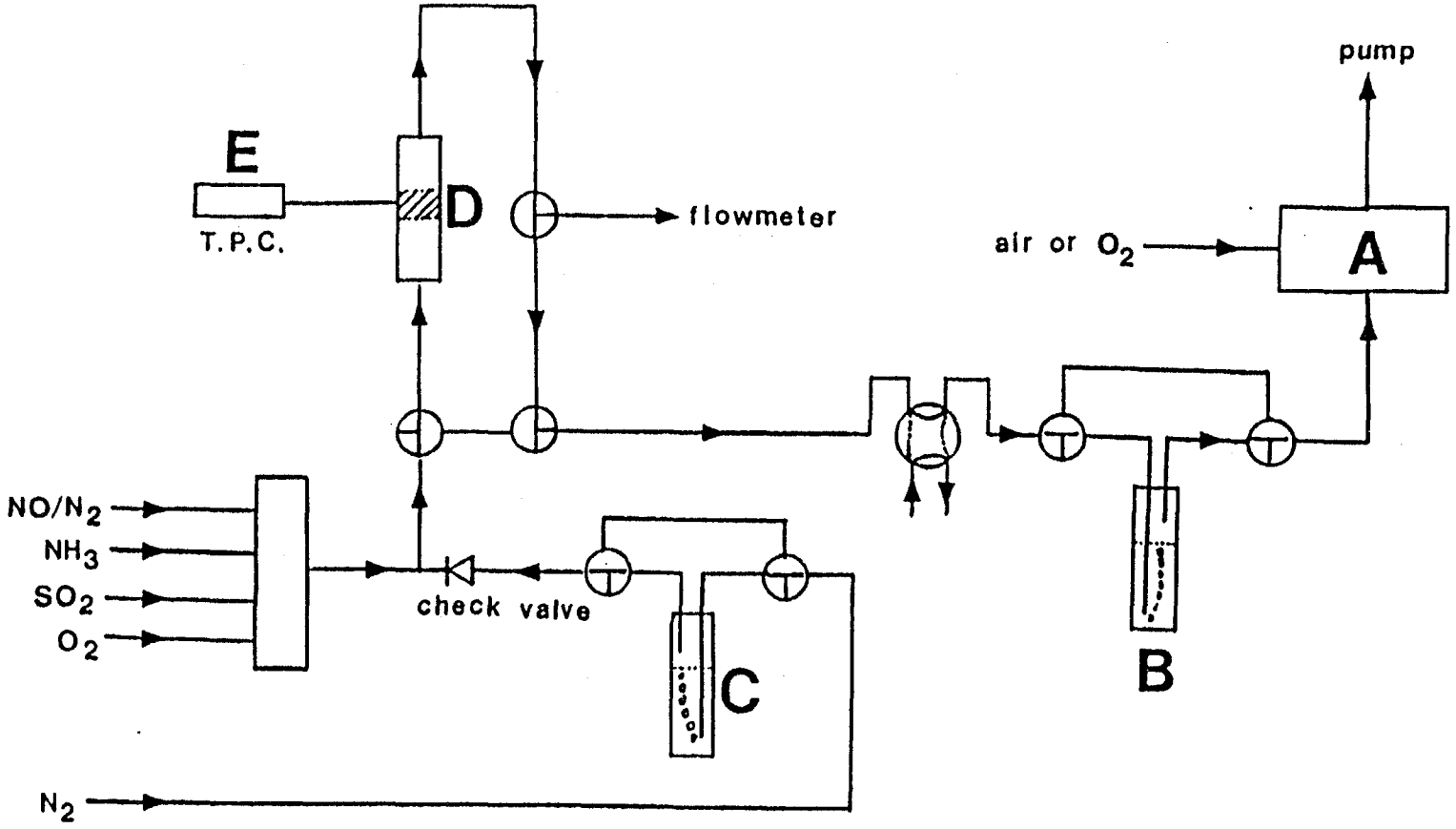

Figure 1. Schematic diagram of experimental SCR reactor: (A) chemiluminescent NO/NO_x analyzer for Reactor 1 or GC/MS analyses for Reactor 2; (B) NH_3 scrubber; (C) water vapor generator; (D) SCR reactor; (E) temperature program controller.

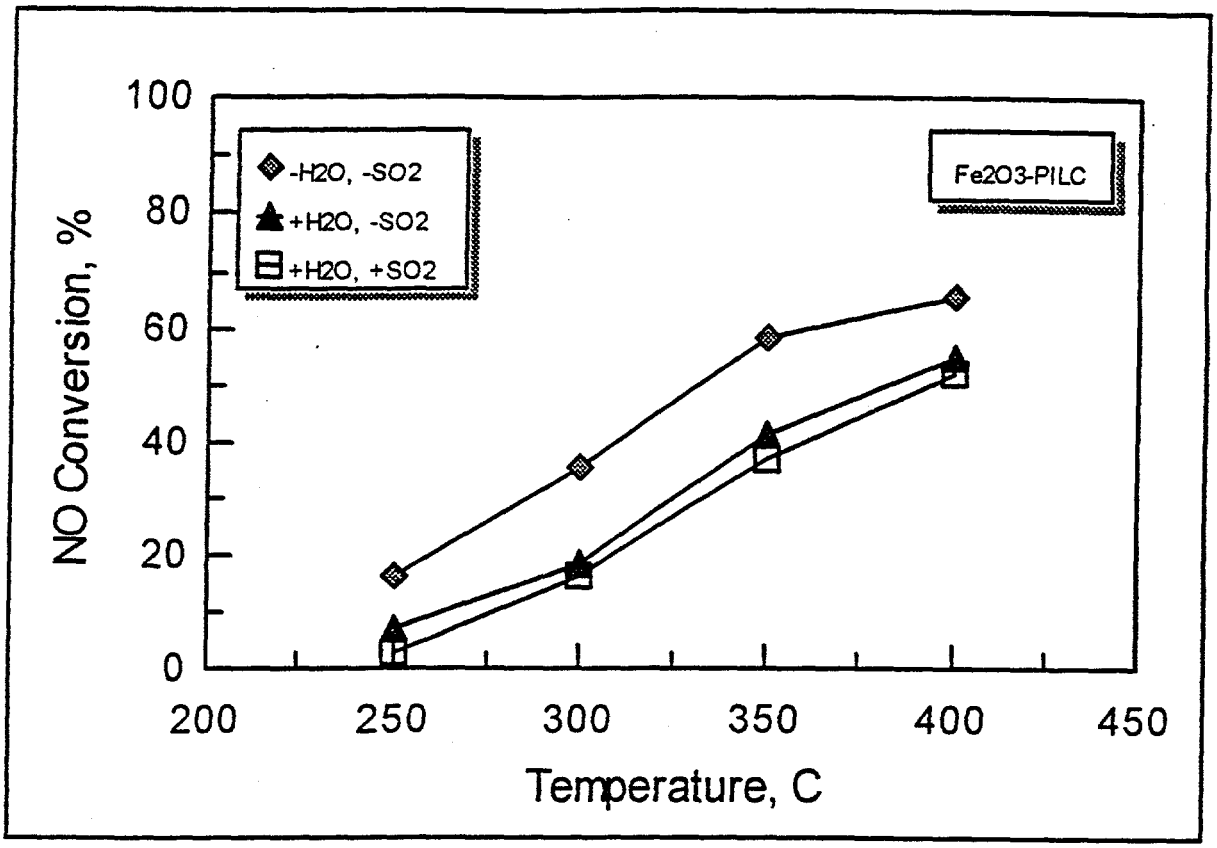

Figure 2. NO conversion on Fe_2O_3-PILC. Reaction conditions: NO = NH_3 = 1,000 ppm, SO_2 = 1,000 ppm, O_2 = 2%, H_2O = 8% (when used), N_2 = balance, total follow rate = 500 ml/min., catalyst = 0.4 gram.

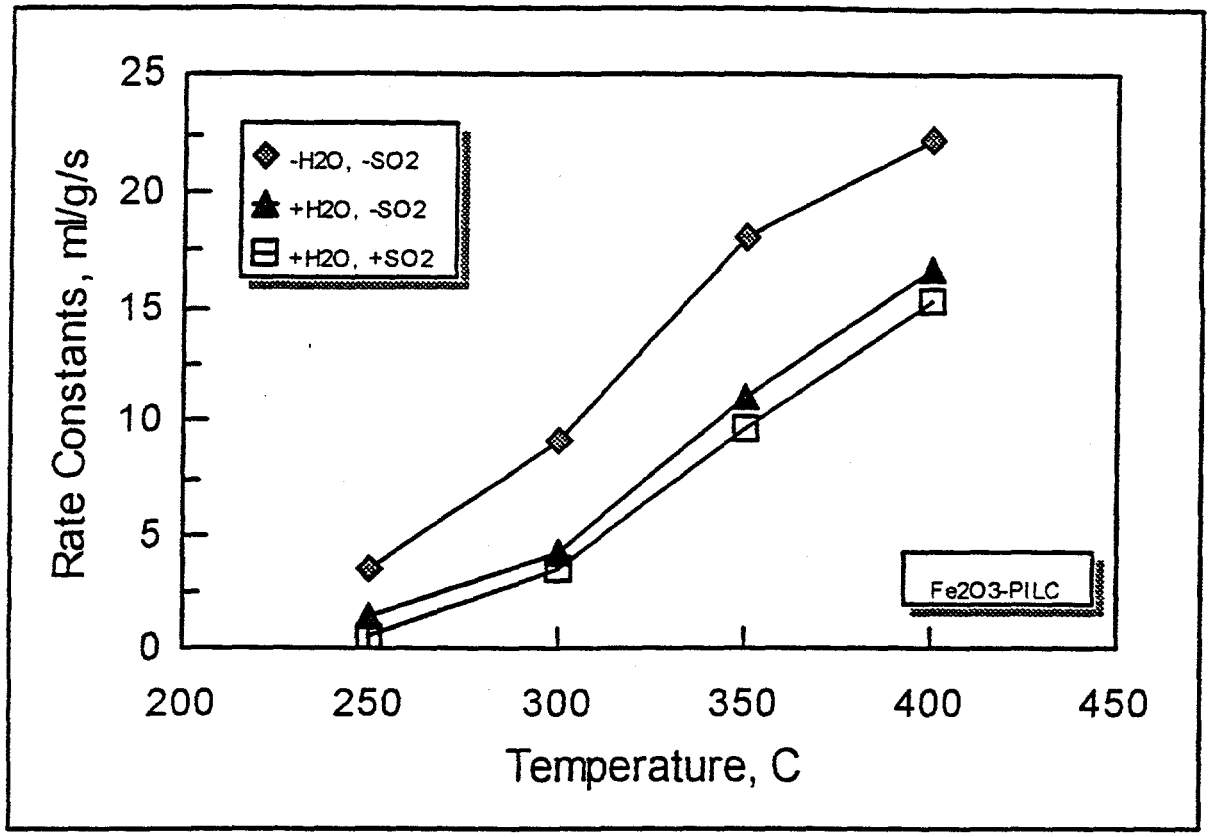

Figure 3. First order rate constant of NO conversion on Fe_2O_3-PILC. Reaction conditions: NO = NH_3 = 1,000 ppm, SO_2 = 1,000 ppm, O_2 = 2%, H_2O = 8% (when used), N_2 = balance, total follow rate = 500 ml/min., catalyst = 0.4 gram.

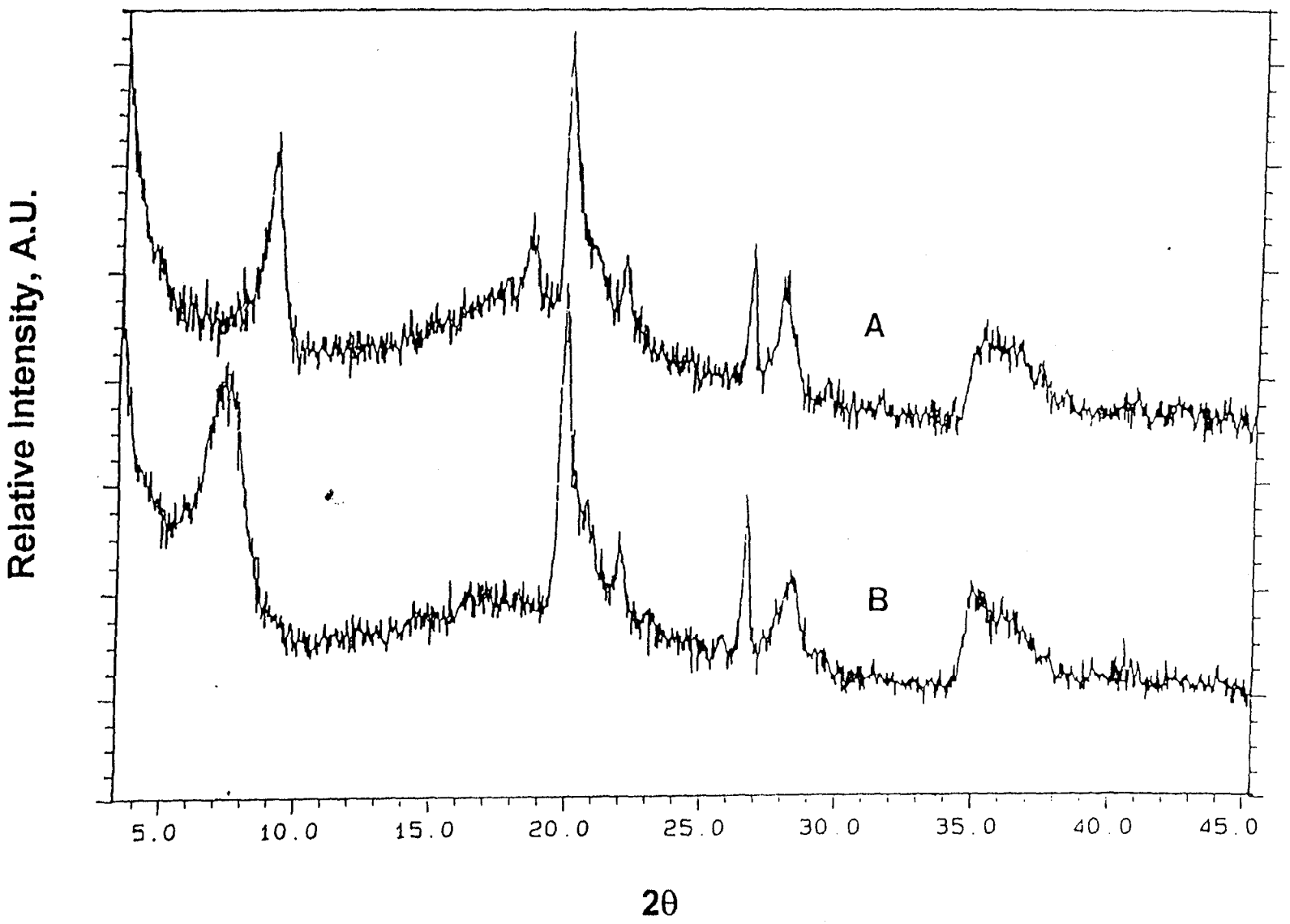

Figure 4. XRD patterns of bentonite (CuKα source). A: No pretreatment; B: Calcined at 300°C for 2 hours.

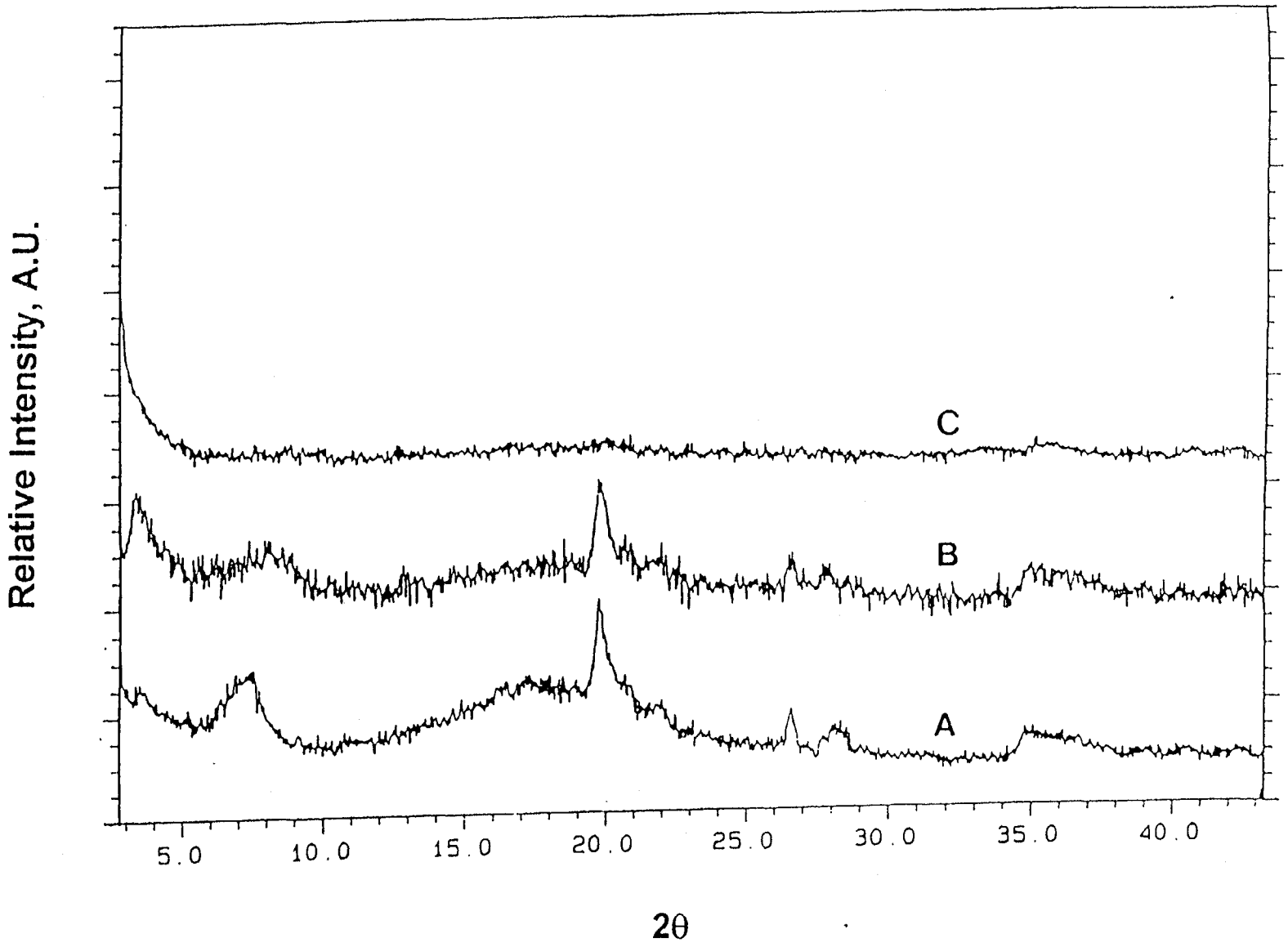

Figure 5. XRD patterns (CuKα source) of bentonite (A); Fe_2O_3-pillared clay (B); and delaminated pillared clay (C).

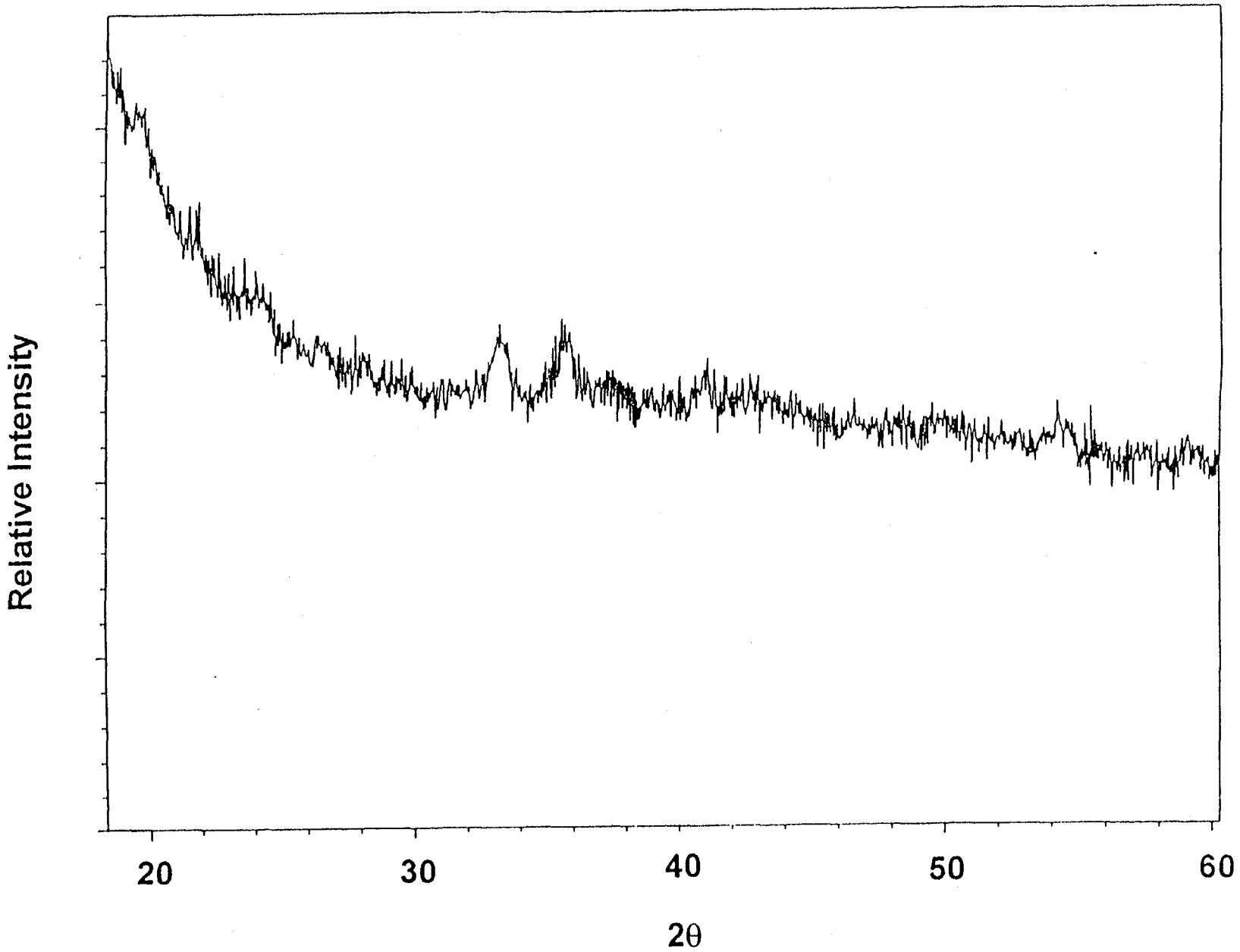

Figure 6. XRD of the delaminated/pillared clay. The broad and weak peaks at 33.43° and 35.79° are reflections of (104) and (110) faces of hematite.

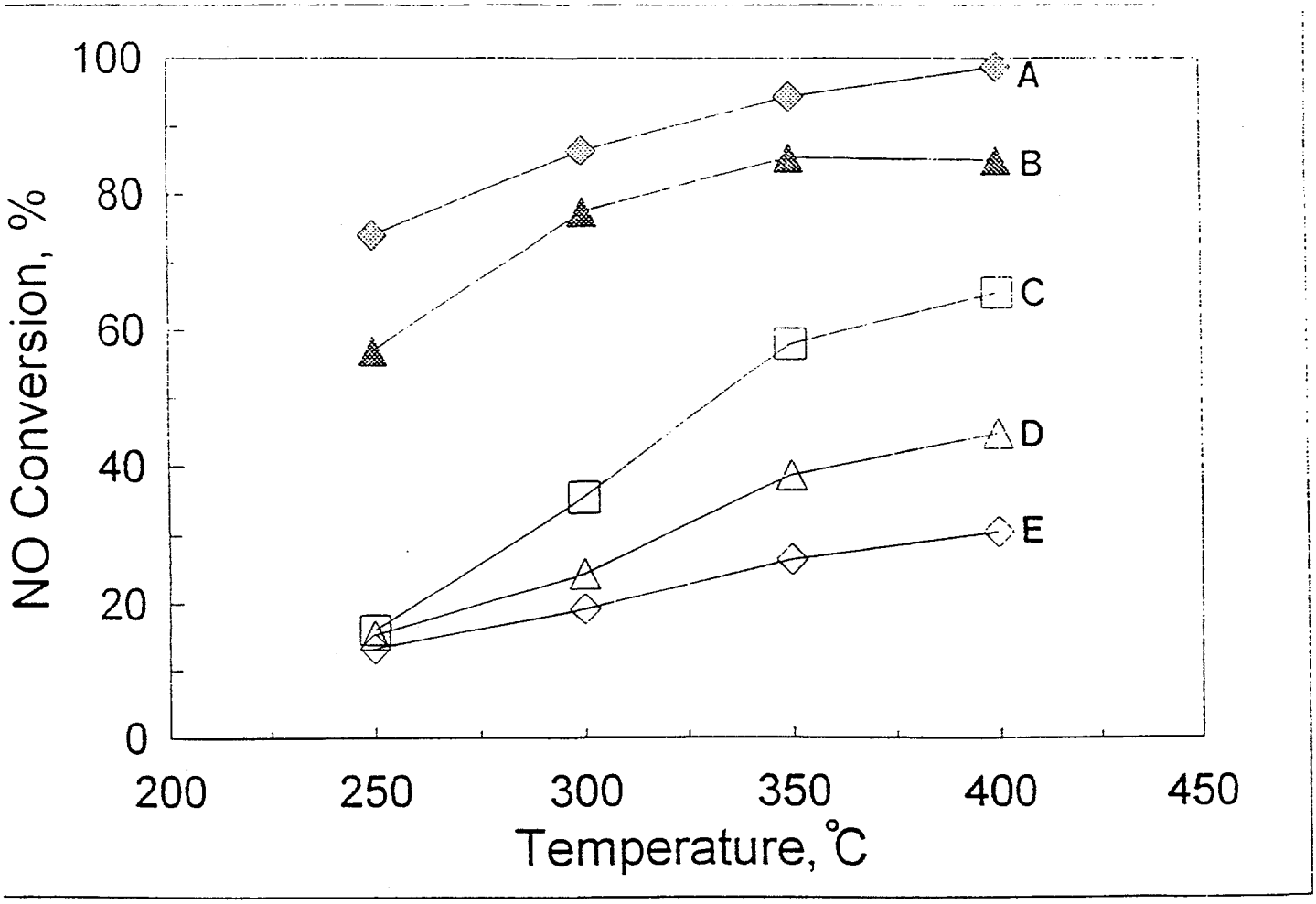

Figure 7. Selective catalytic reduction of NO with NH_3 on different catalysts. Reaction conditions: NO = NH_3 = 1,000 ppm, O_2 = 2%, N_2 balance, total flow rate = 500 ml/min., catalyst weight = 0.4 gram. A: delaminated pillared clay, B: $V_2O_5 + WO_3/TiO_2$, C: Fe_2O_3-pillared clay, D: Fe_2O_3/Al_2O_3 and E: Fe_2O_3/TiO_2.

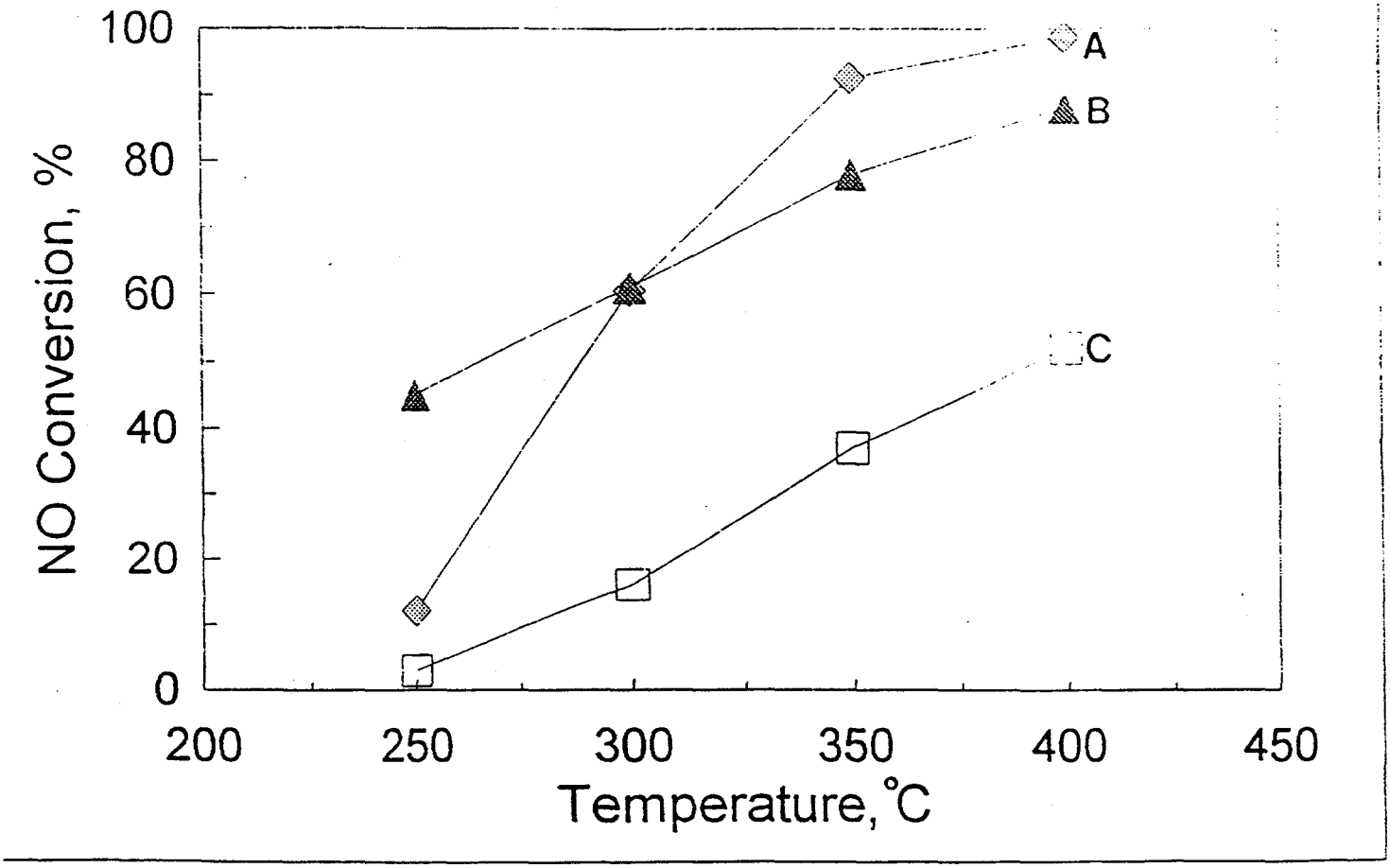

Figure 8. Selective catalytic reduction of NO with NH_3 on different catalysts. Reaction conditions are the same as in Fig. 4 except H_2O (8%) and SO_2 (500 ppm) are added. A: delaminated pillared clay, B: V_2O_5 + WO_3/TiO_2 and C: Fe_2O_3-pillared clay.

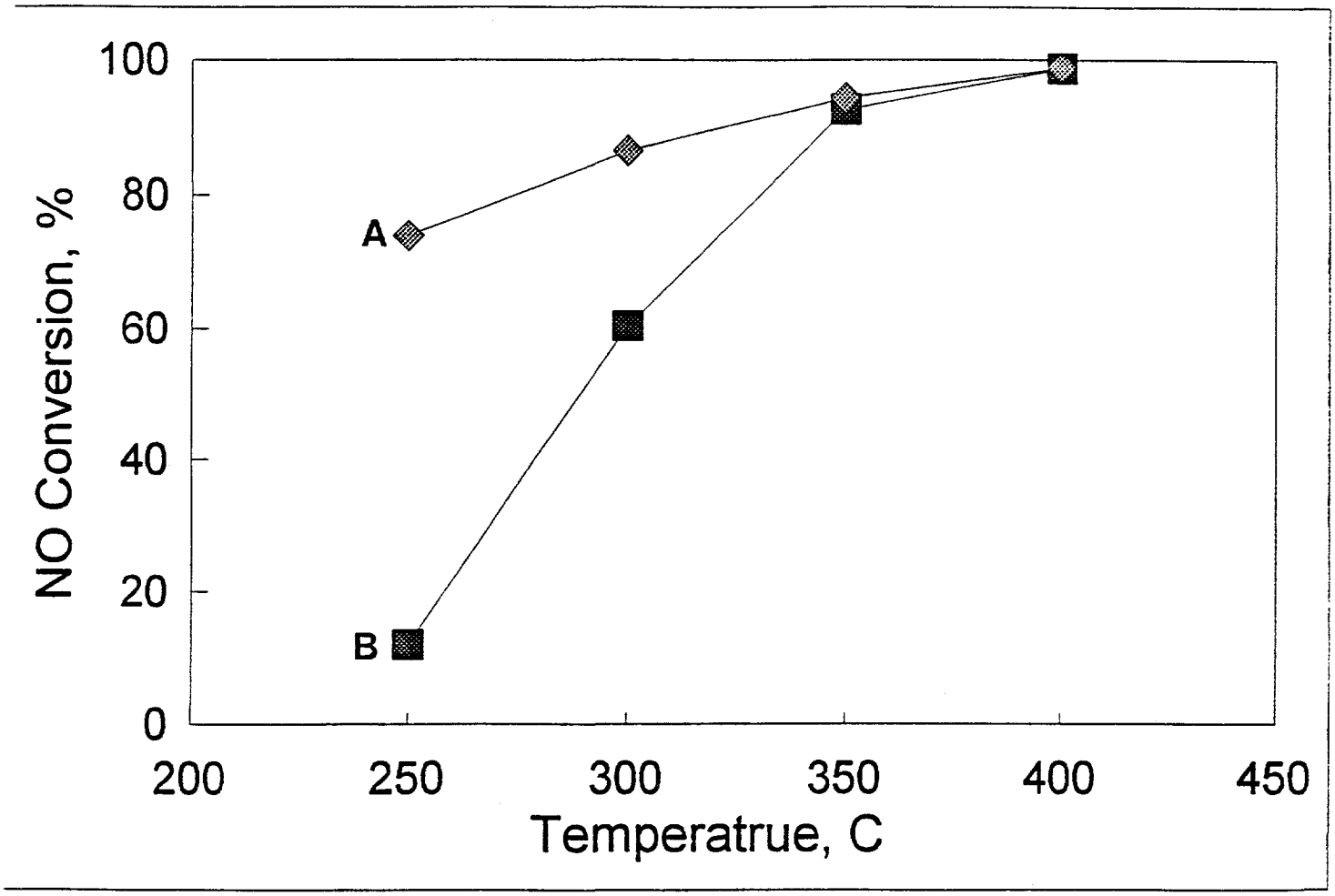

Figure 9. Selective catalytic reduction of NO with NH_3 on delaminated Fe_2O_3 pillared clay. Reaction conditions are the same as in Fig. 4. A: Without SO_2 and H_2O vapor addition. B: With SO_2 (500 ppm) and H_2O (8%) addition.

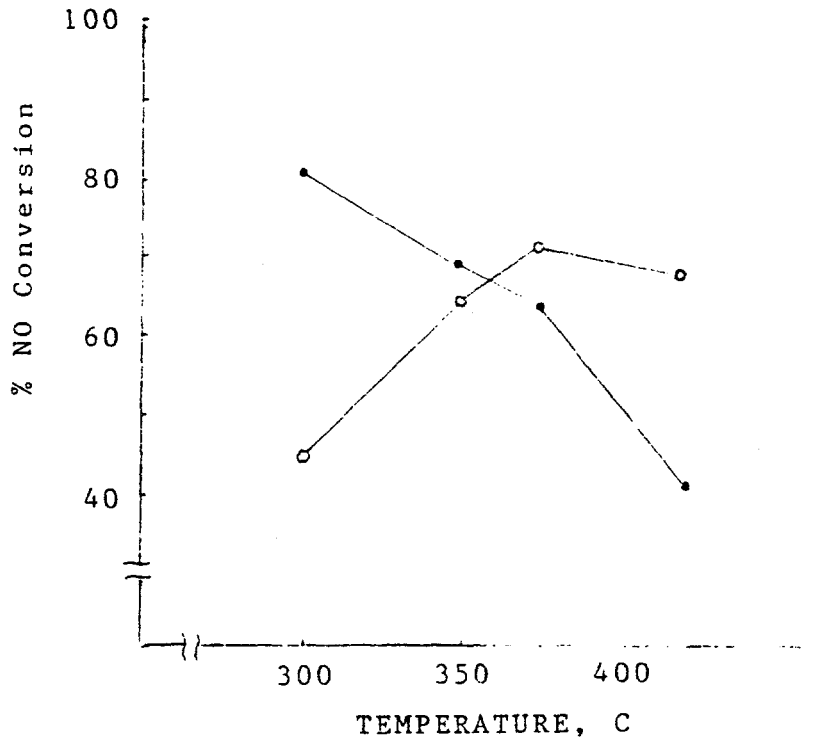

Figure 10. Effect of Cr_2O_3 doping on the SCR activity of Fe_2O_3 PILC (Sample 613). Open Circles: Delaminated PILC Sample 613. Dots: With 2.5% Cr_2O_3 doped in Sample 613. The SCR reaction conditions are given in Section B1.

Figure Captions

Figure 11. SCR of NO by ammonia over Fe-Bentonite pillared clay at (a) 4 0% O_2; (b) 2.0% O_2; (c) 0.4% O_2; and (d) without O_2. Catalyst: 0.4 gram, 100-140 mesh, No. 905 catalyst. Feed stream: 1,000 ppm NO, 1,000 ppm NH_3, and 0-4.0% O_2 in N_2, GHSV = 75,000 h^{-1}.

Figure 12. SCR of NO by ammonia over Fe-Bentonite catalysts with particle size fractions: (a) 20-35 mesh; (b) 35-60 mesh; (c) 80-100 mesh; and (d) 100-140 mesh. Catalyst: 0.4 gram No. 901 catalyst. Feed stream: 1,000 ppm NO, 1,000 ppm NH_3, and 0.3% O_2 in N_2, GHSV = 75,000 h^{-1}.

Figure 13. SCR of NO by ammonia over Fe-Bentonite doped with (a) 20% Cenum oxide, and (b) without Cerium oxide. Feed stream: 1,000 ppm NO, 1,000 ppm NH_3, and 4.0% O_2 in N_2. GHSV = 75,000 h^{-1}.

Figure 11. Effect of O_2 on NO Conversion

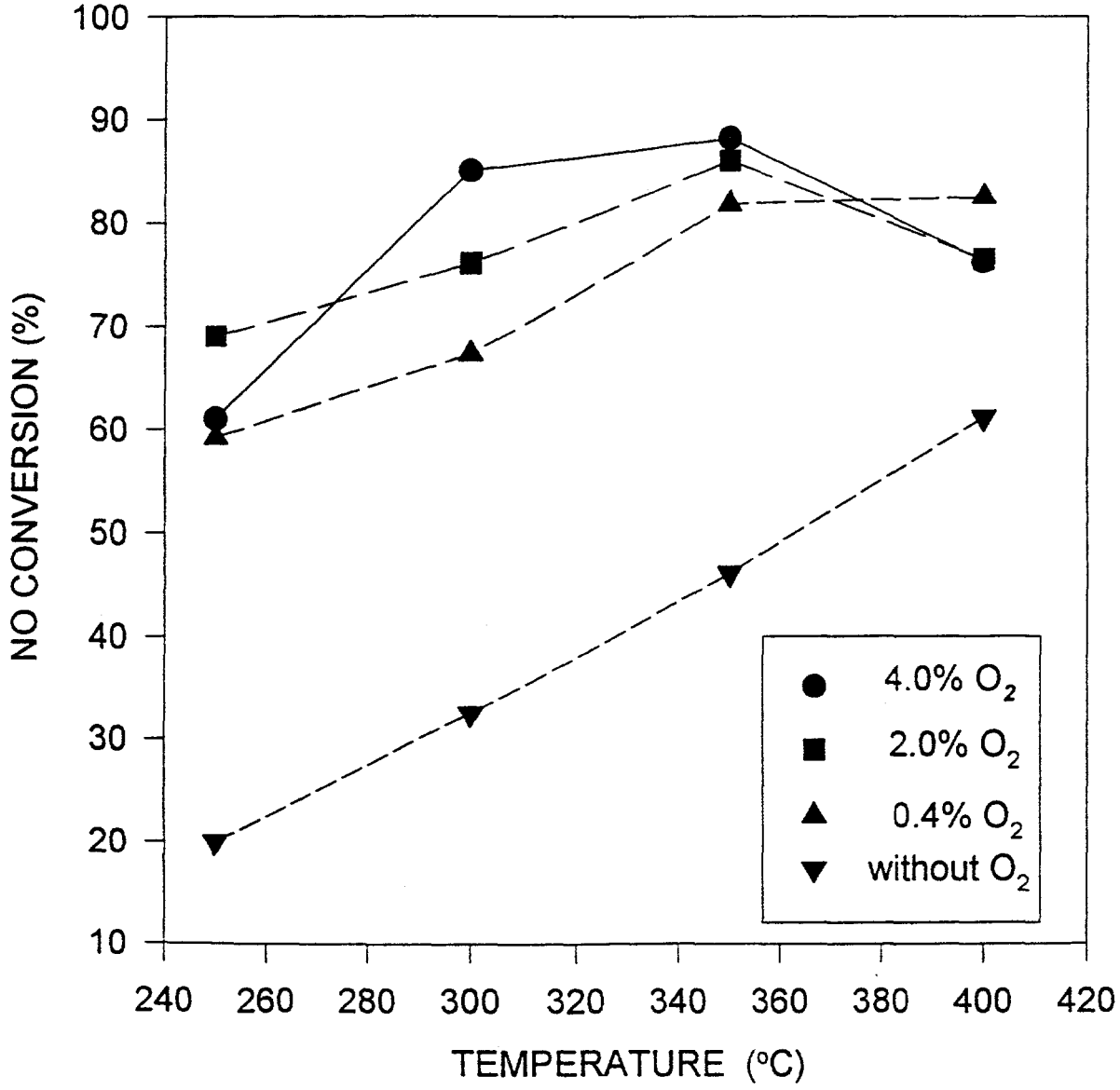

Figure 12. Effect of Internal Diffusion on NO Conversion

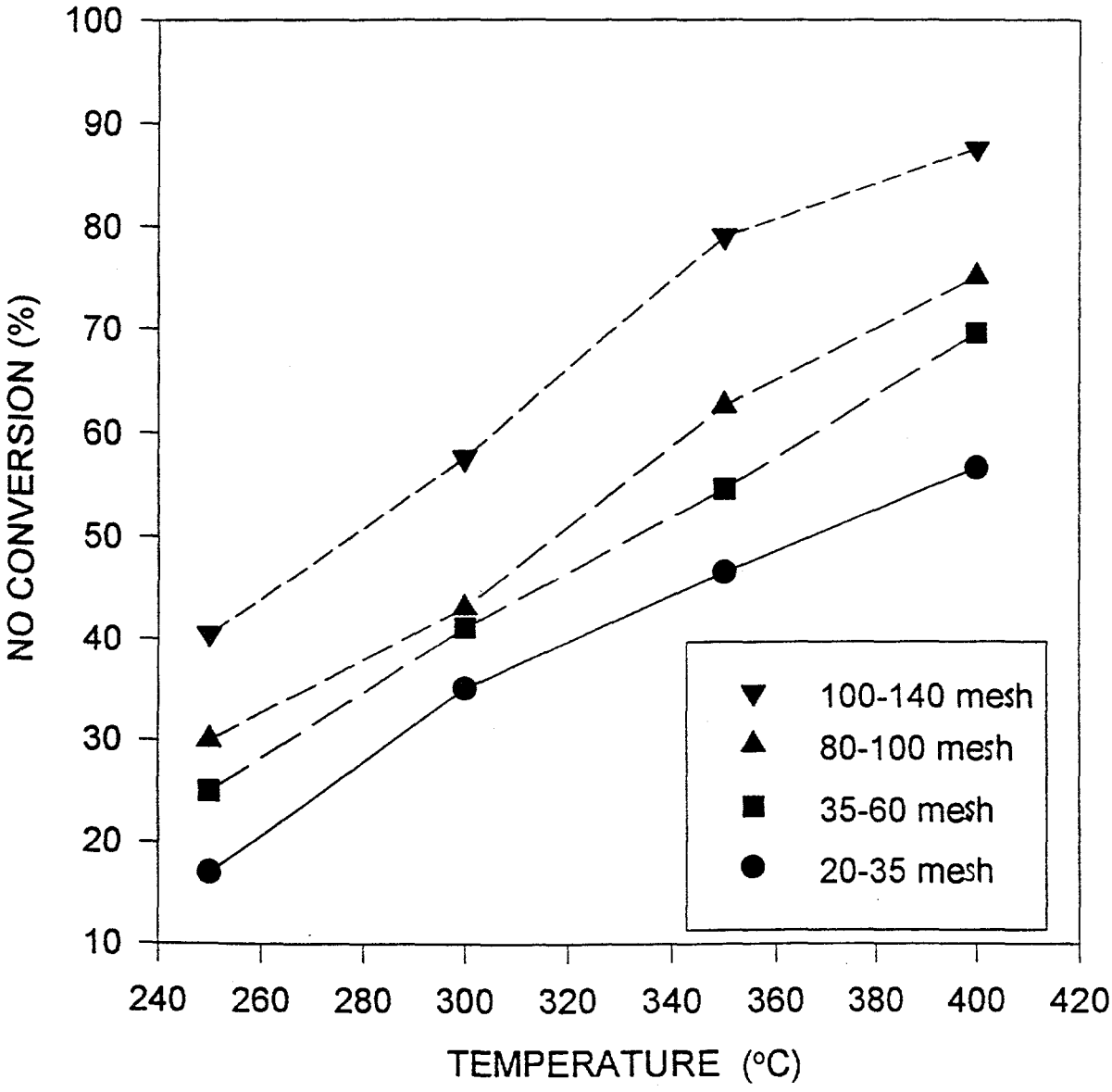

Figure 13. Promoting Effect of CE On NO converison

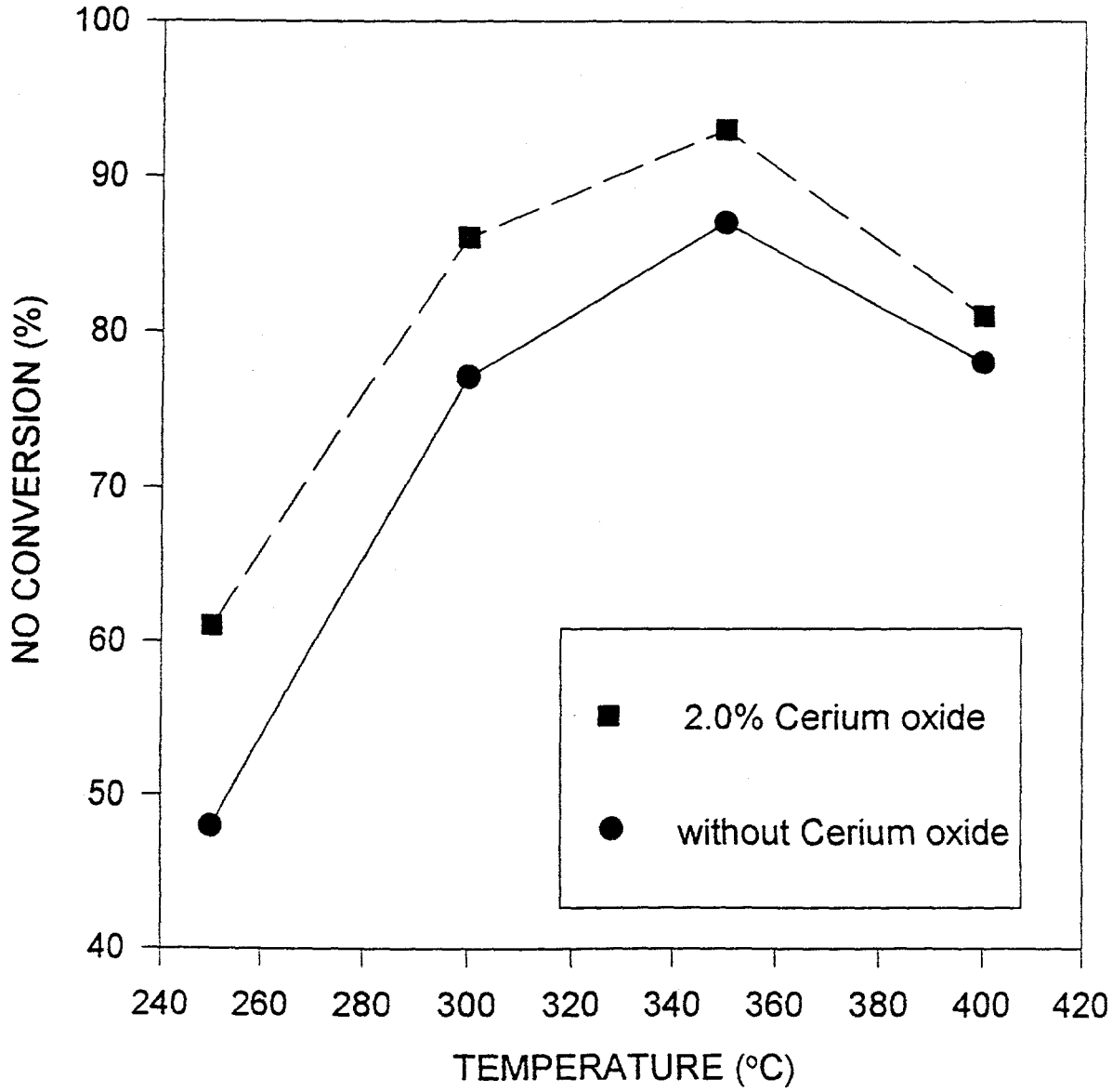

Figure 14. Poisoning Effect of Alkali Metal

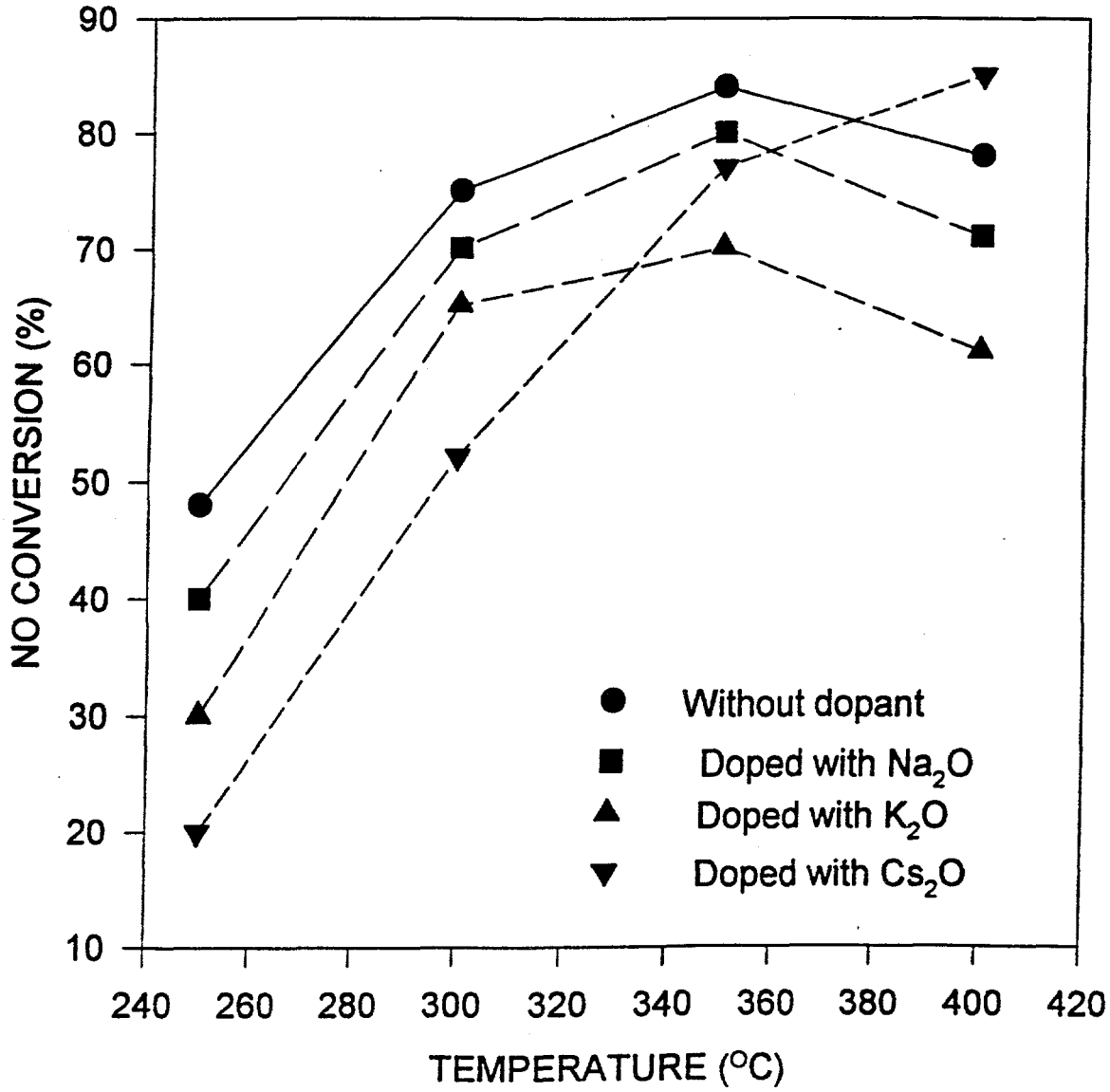

Figure 15. Effect of SO_2 and H_2O on NO Converison

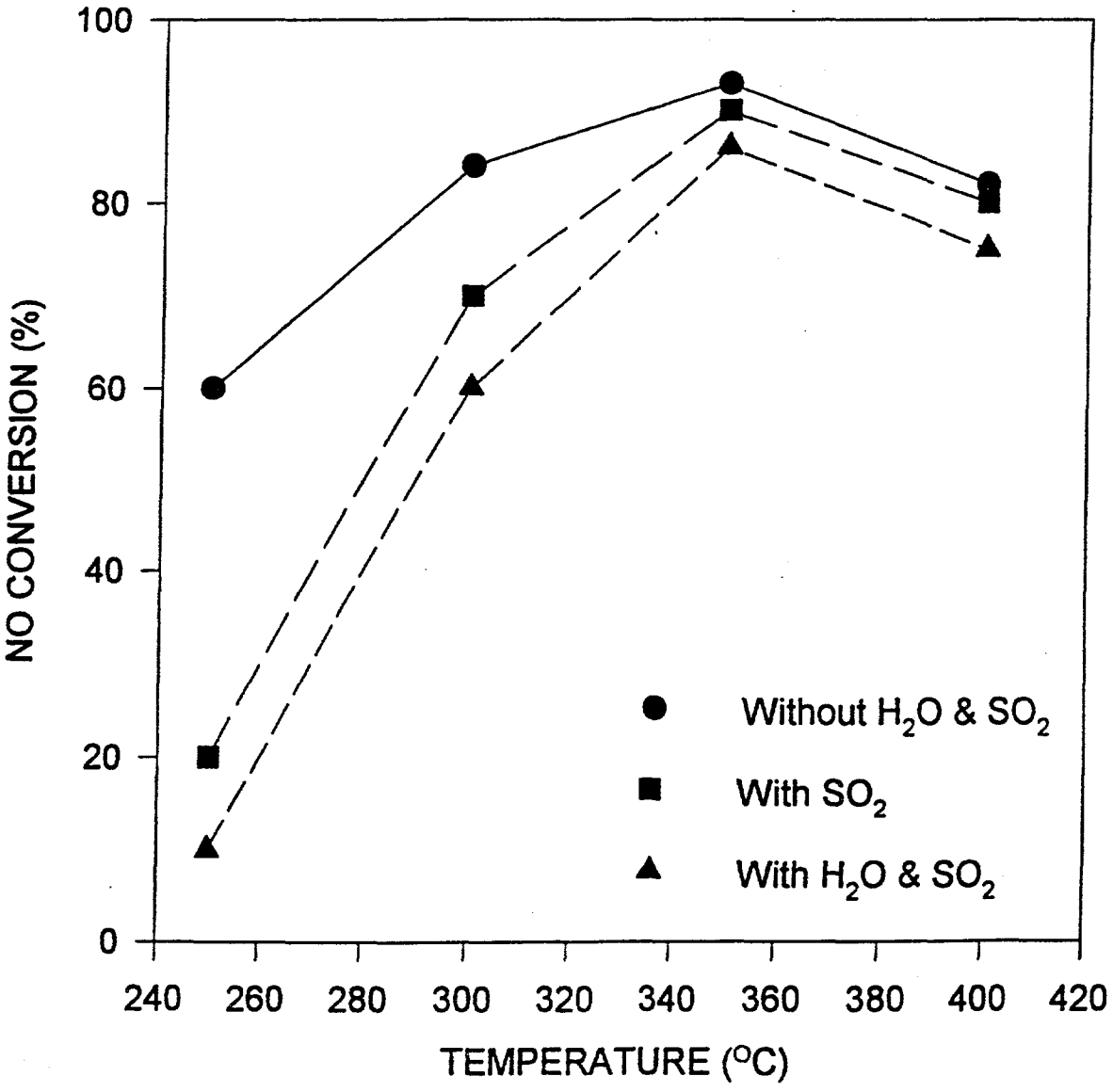

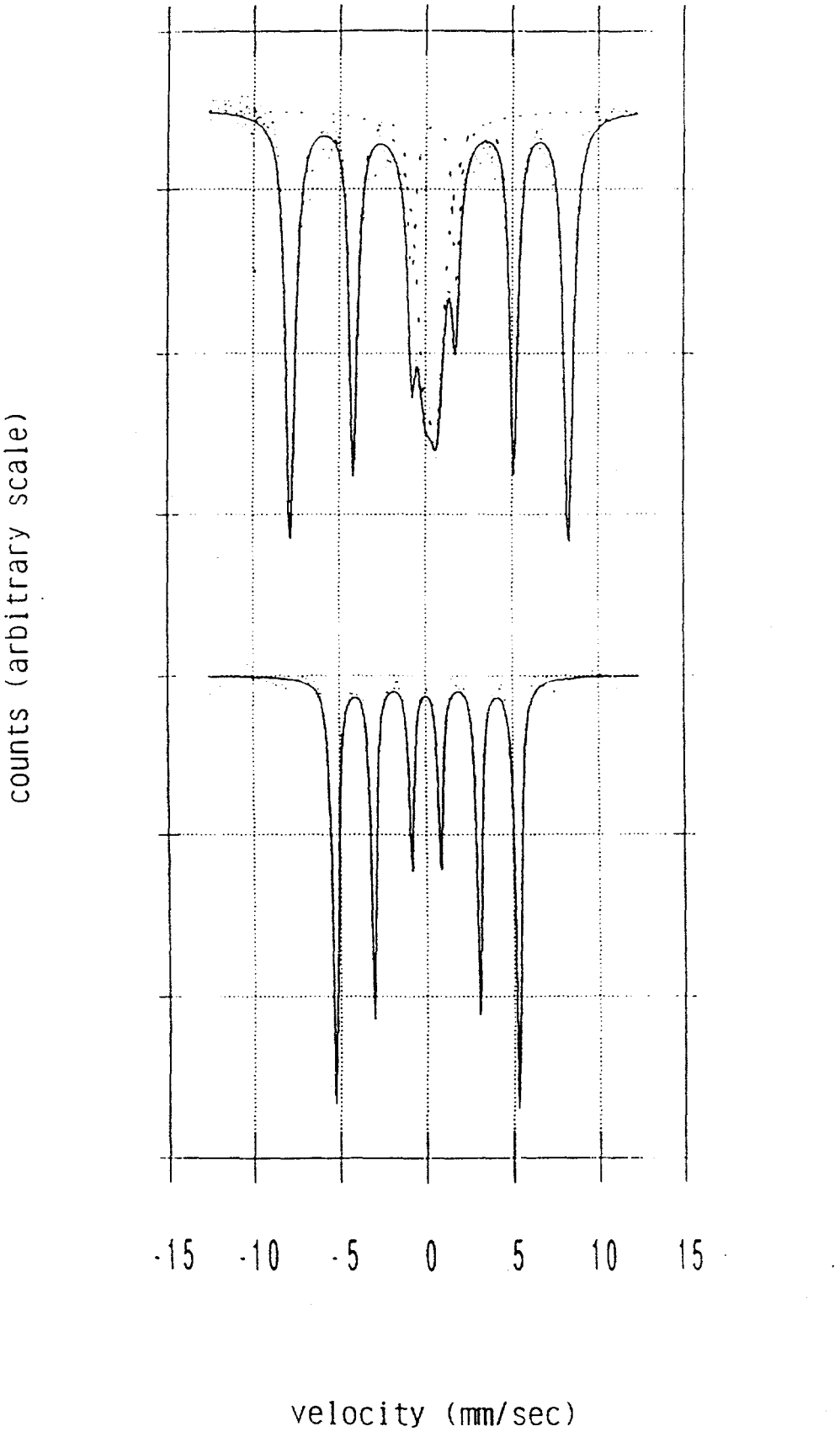

Figure 16. Mössbauer spectrum of delaminated/pillared clay in the range of +/- 10 mm/sec, shown relative to iron foil.

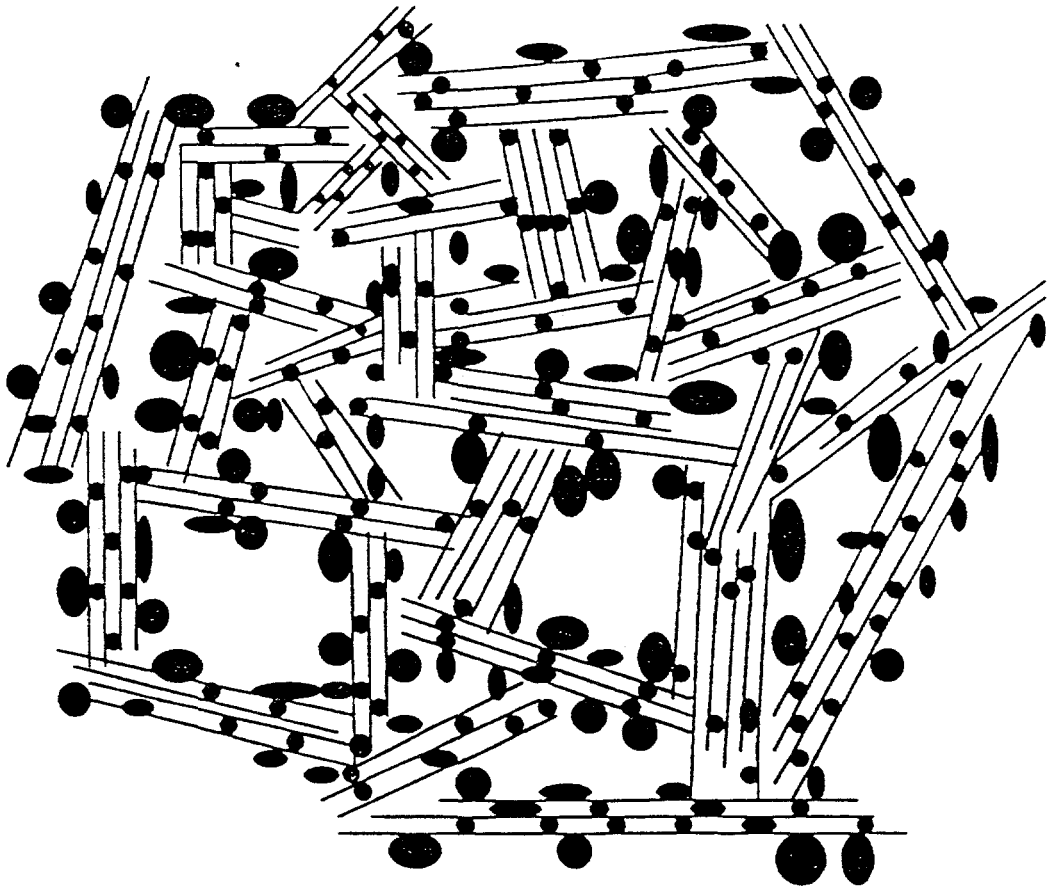

Figure 17. Schematic representation of the delaminated/pillared clay containing iron oxide particles.

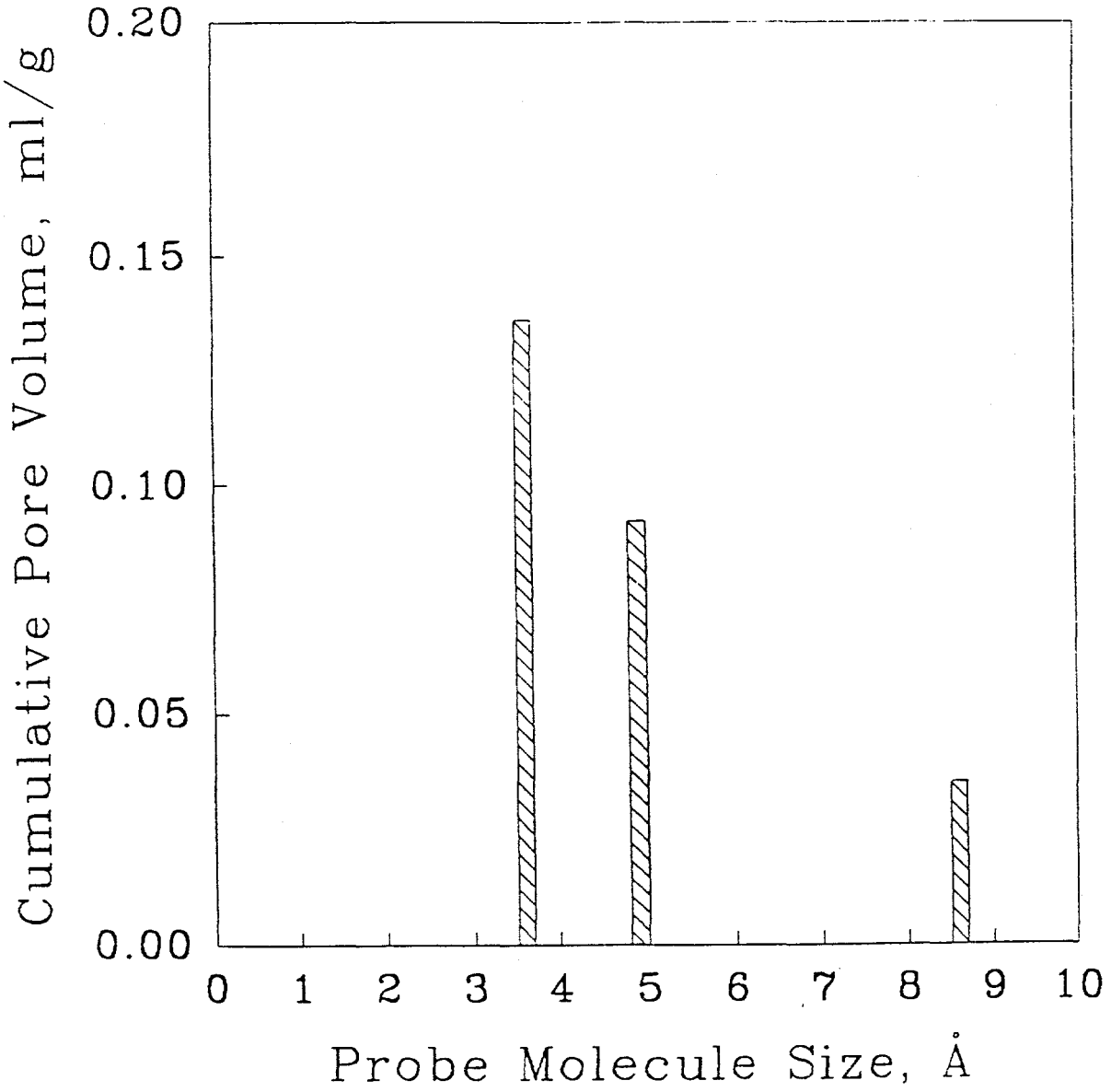

Figure 18. Cumulative micropore volume as a function of pore dimension measured by micropore filling with probe molecules (N_2 = 3.6 Å, n-hexane = 4.9 Å and 1,3,5-trimethyl benzene = 8.6 Å).

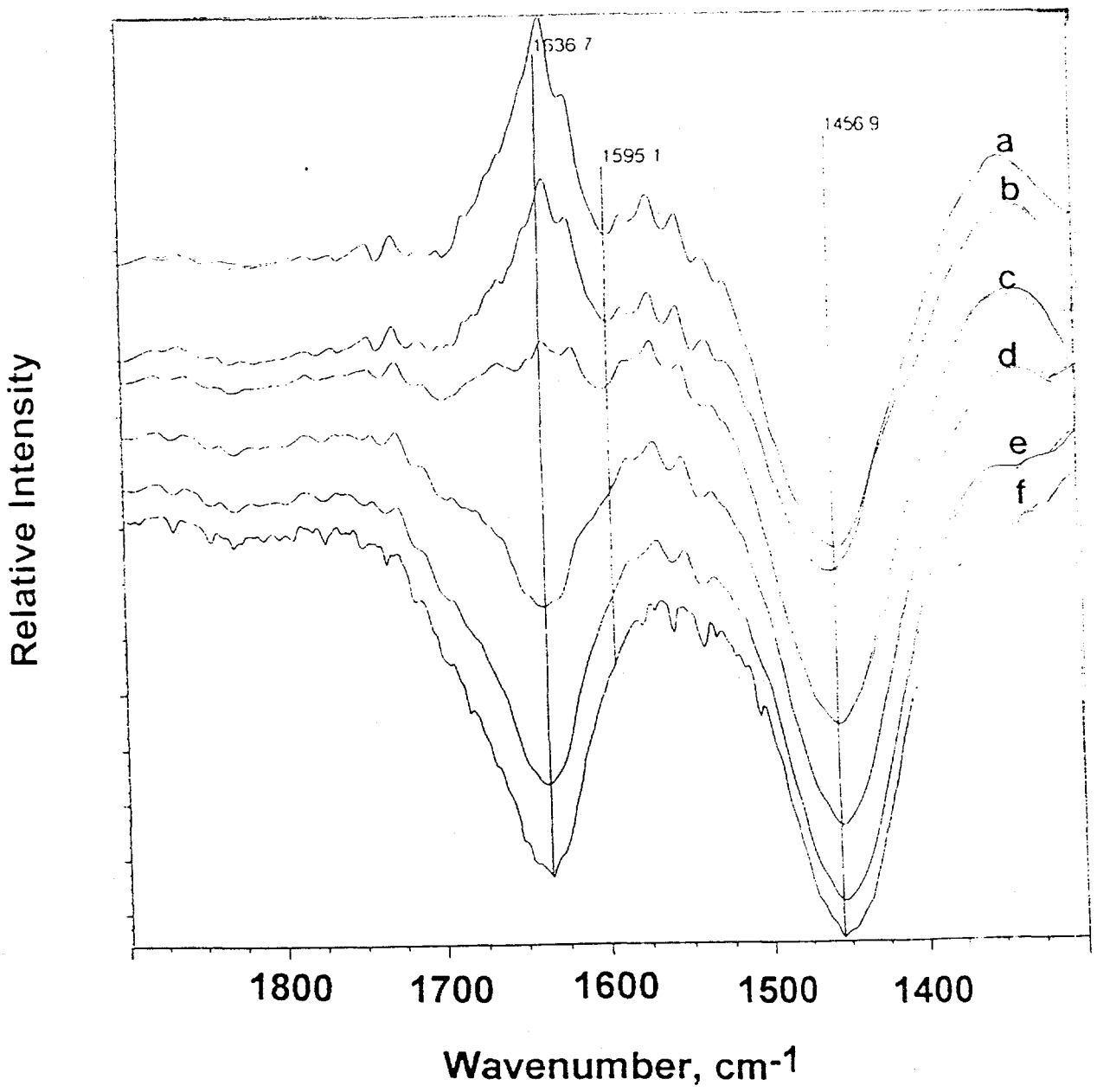

Figure 19. FT-IR spectra of ammonia adsorbed on delaminated Fe_2O_3 pillared clay (a). (b)-(f) are after exposure to 2% H_2O, at one-minute successive time intervals. All spectra are taken at room temperature, and ratioed against the sample before NH_3 exposure (but after calcination).

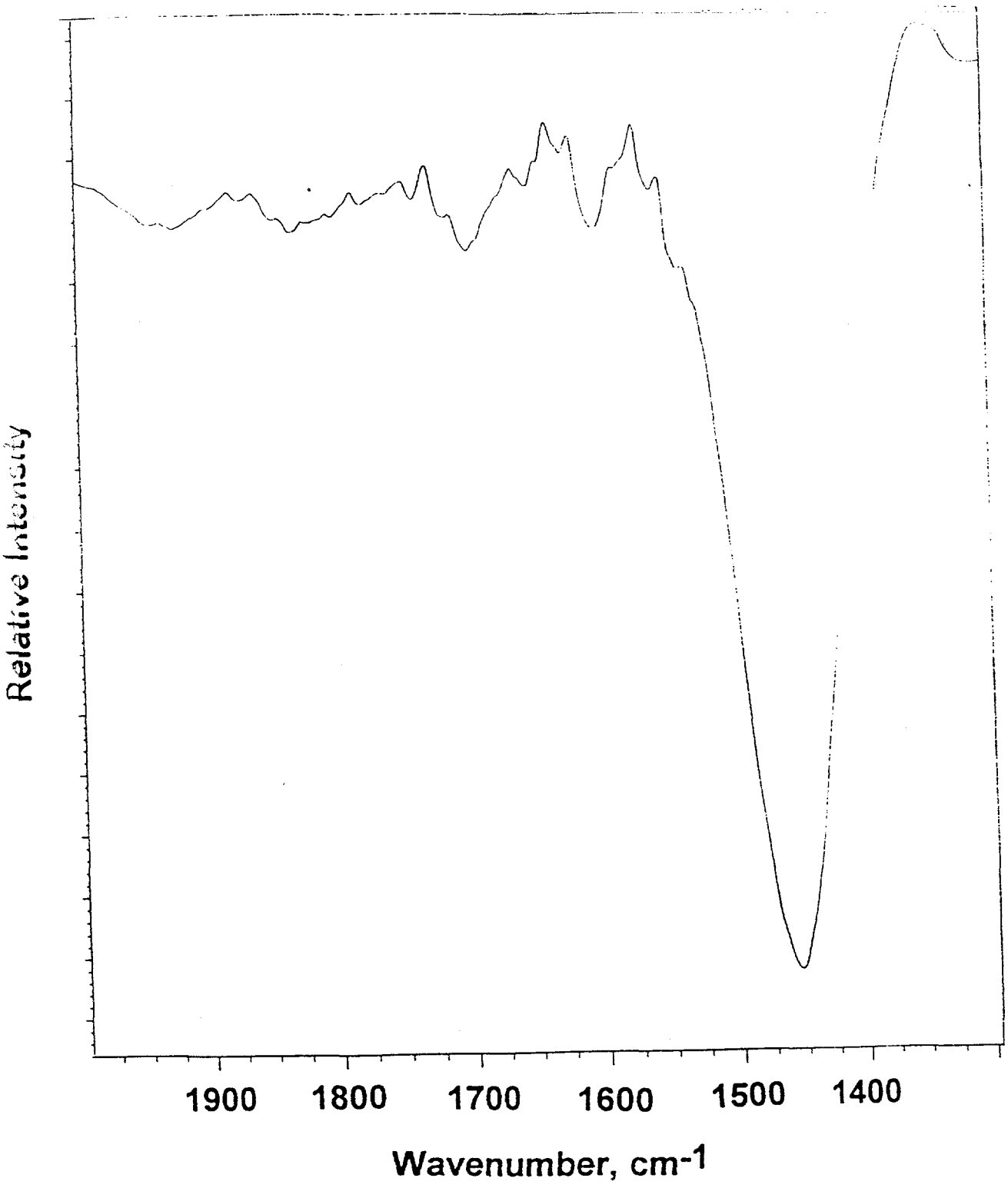

Figure 20. FT-IR spectra of ammonia adsorbed on delaminated/pillared clay at 150°C.

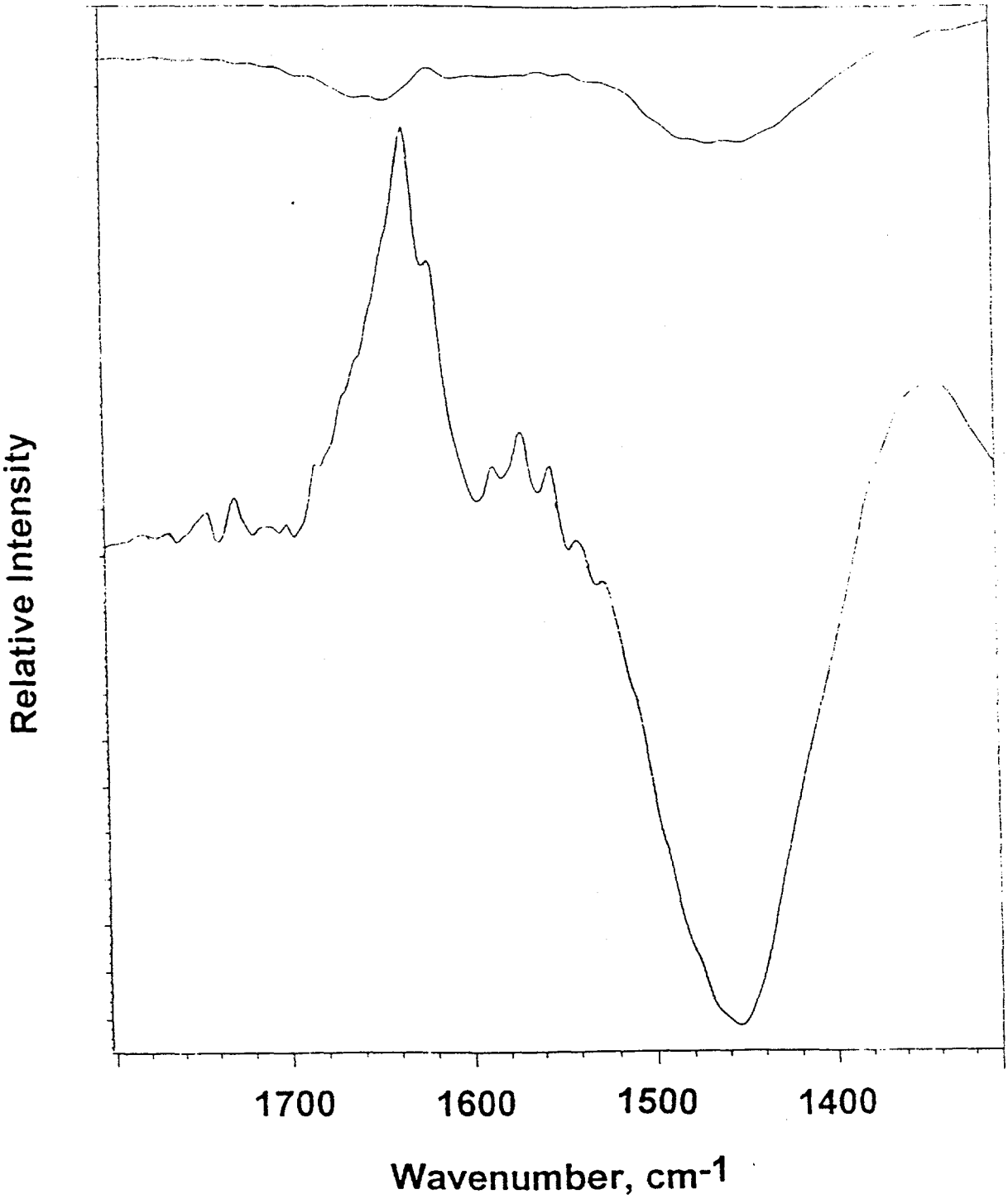

Figure 21. FT-IR spectra of ammonia adsorbed on montmorillonite (top) and delaminated/pillared clay at room temperature.

Figure Captions

Figure 22. Temperature programmed desorption profile of NO_x from montmorillonite clay (absorbed at room temperature, 1,000 ppm NO, 0.4 g clay, N_2 flowrate = 350 ccSTP/min, heating rate = 10°C).

Figure 23. Temperature programmed desorption profile of NO_x from montmorillonite clay (conditions were the same as in Figure 2 except the adsorption was in the presence of 2% O_2).

Figure 24. Temperature programmed desorption profile for NO_x from delaminated Fe_2O_3 pillared clay (conditions were the same as that in Figure 3, also in 2% O_2). $NO_x = NO + NO_2$.

Figure 25. TPD profiles for delaminated Fe_2O_3 -pillared clay with NO adsorbed at 400°C followed by purge with NH_3 and then N_2 (both at 400°C). (See text for detailed conditions.) The top profile is from first temperature ramp and the lower profile is from the third ramp, with no NO or NH_3 treatment between successive TPD runs.

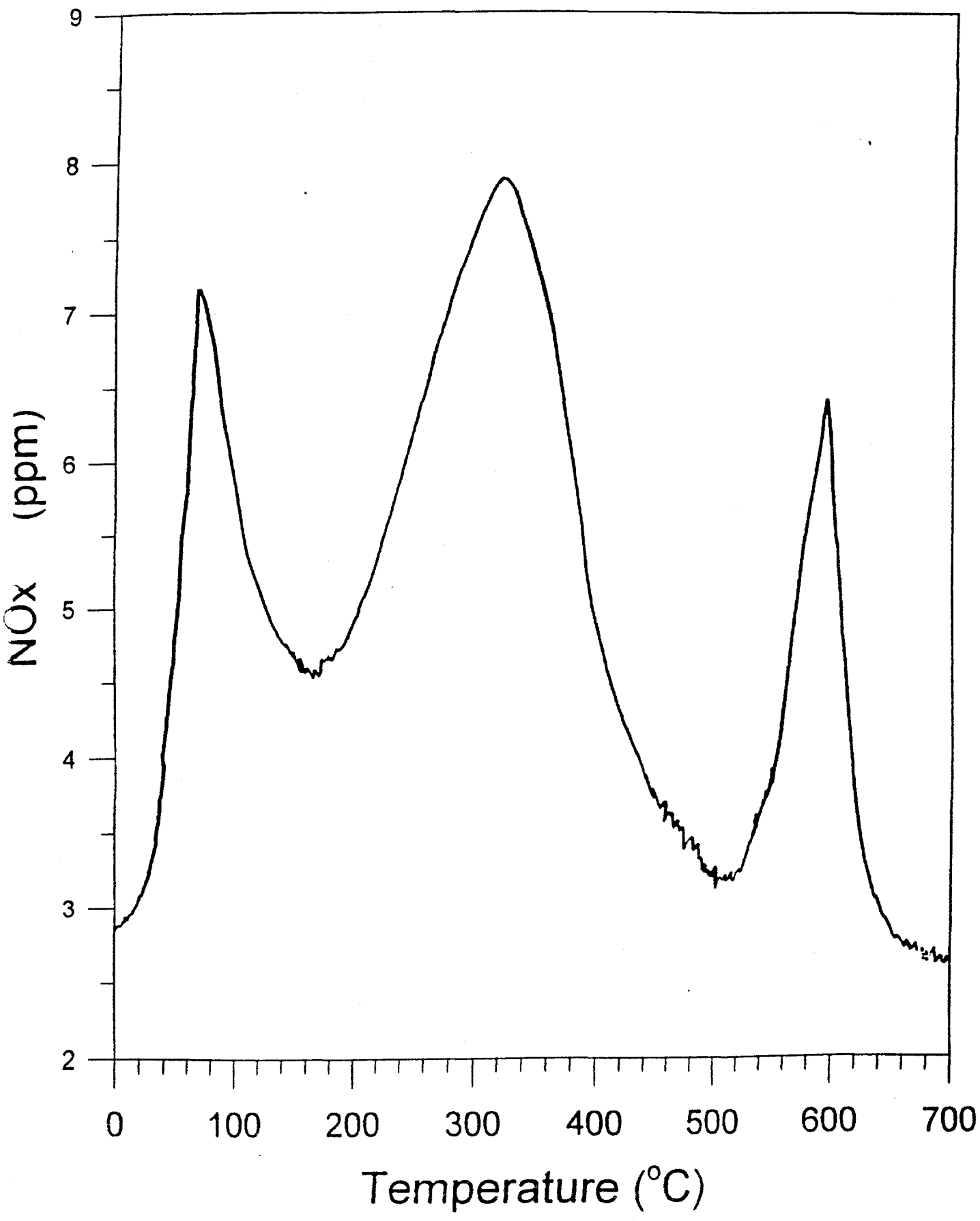

Figure 22

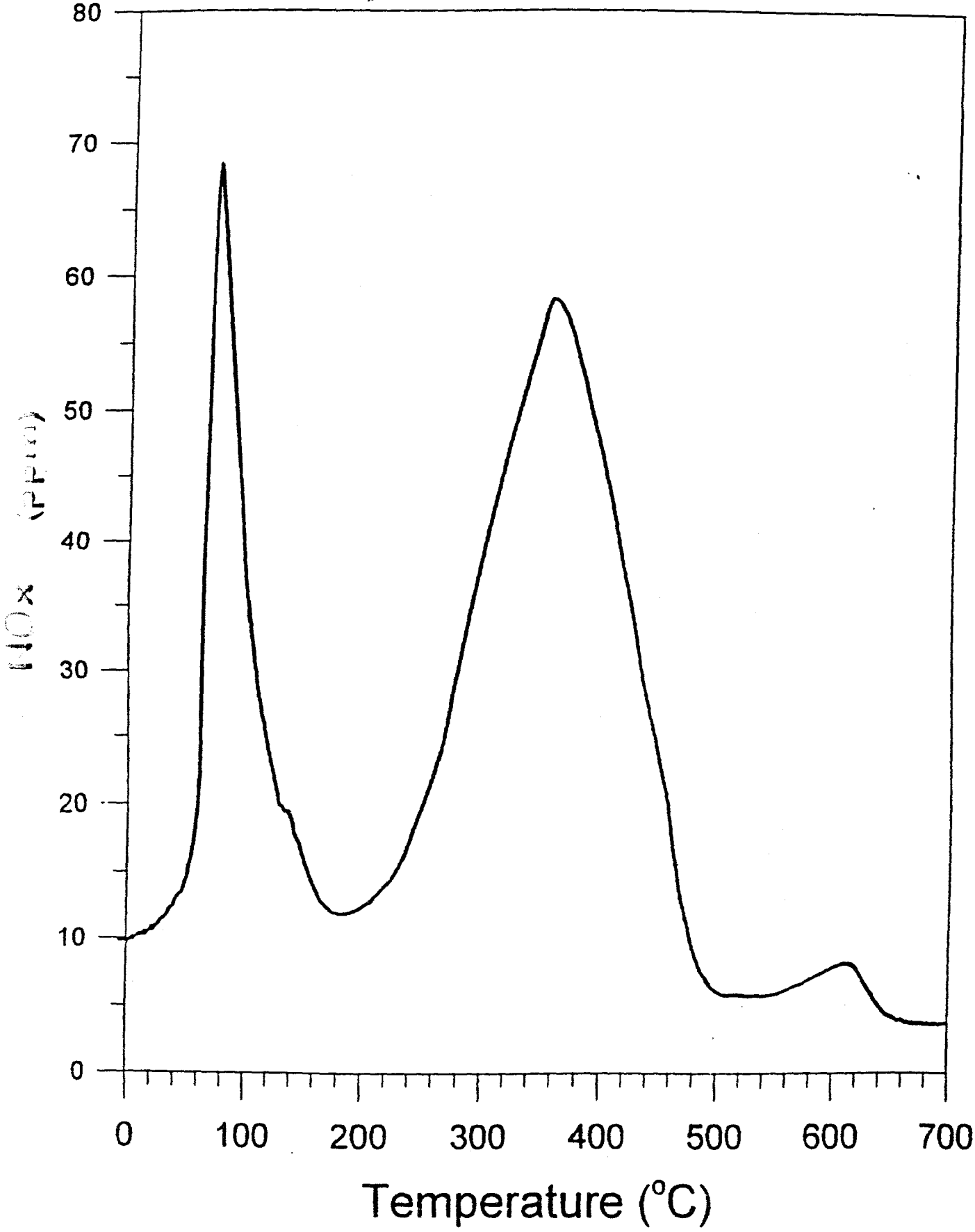
80
70
60
50
40
30
20
10
0
0
100
200
300
400
500
600
700
Temperature (°C)

Figure 23

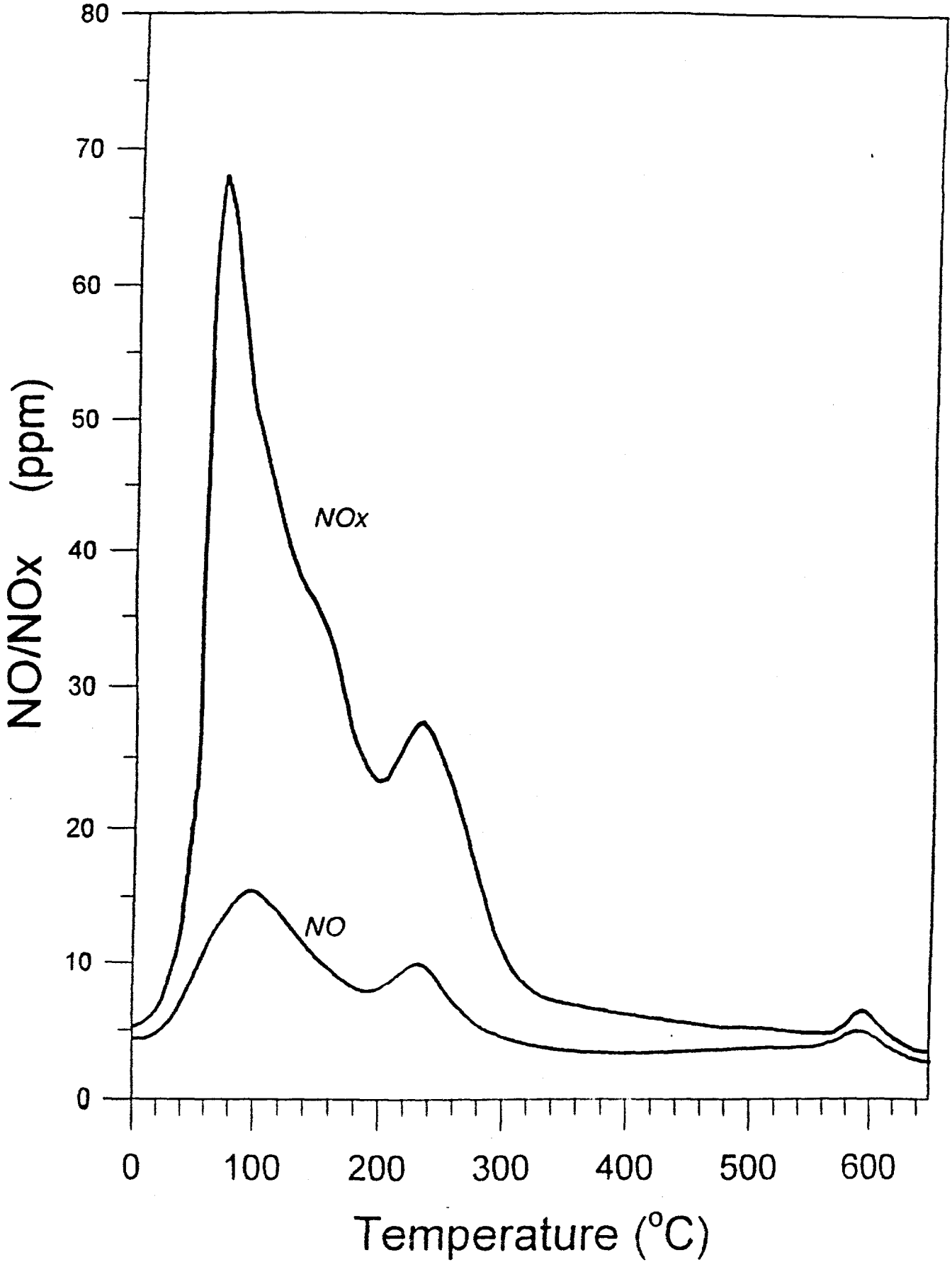
80
70
60
50
40
30
20
10
0
NO/NOx (ppm)
NOx
NO
0
100
200
300
400
500
600
Temperature (°C)

Figure 24

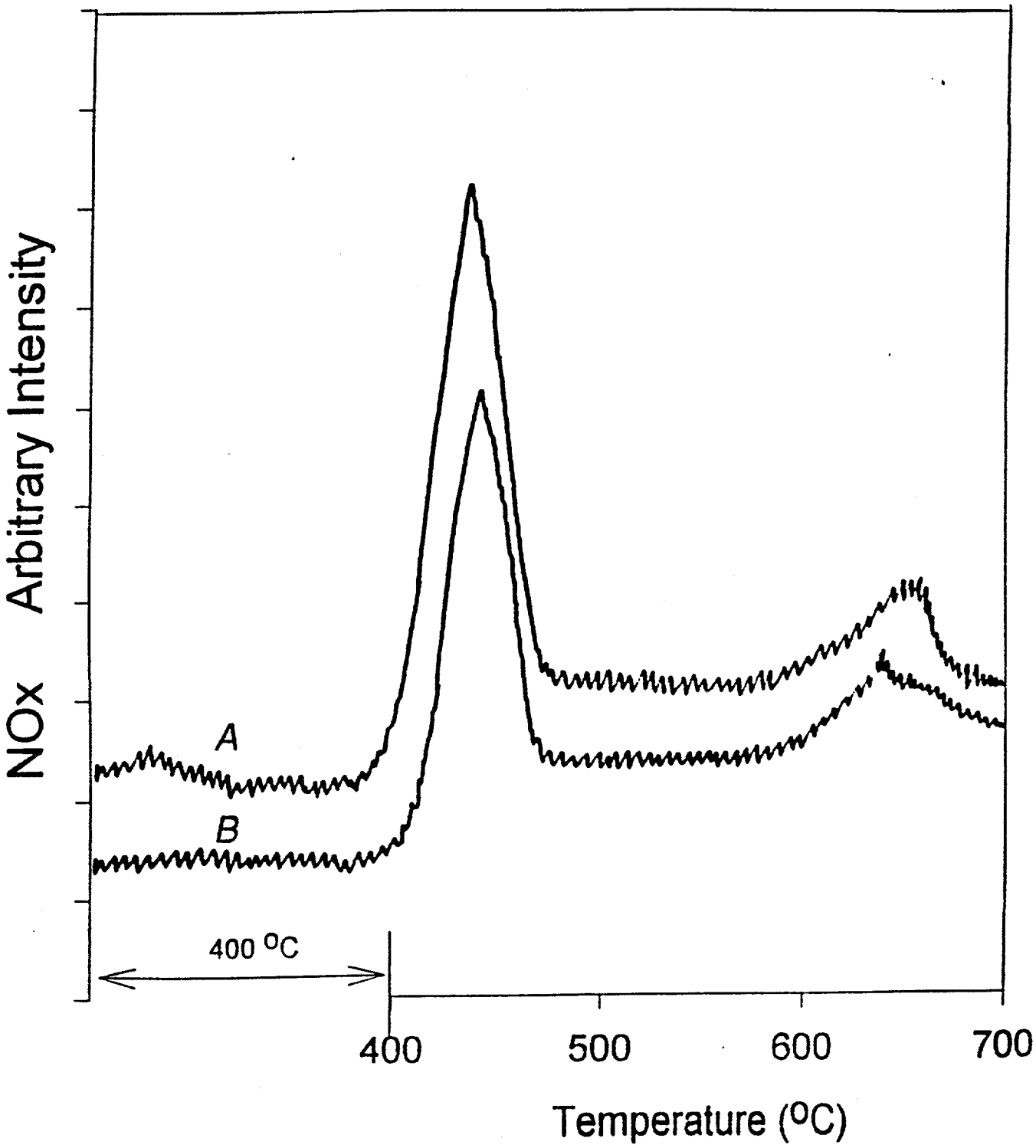
NOx Arbitrary Intensity
A
B
400 °C
400
500
600
700
Temperature (°C)

Figure 25

Figure Captions

Figure 26. Comparison of activities for SCR by NH_3 between WO_3 + V_2O_5/TiO_2 and Fe^{3+} exchanged TiO_3 pillared clay. Reaction conditions: NO = NH_3 = 1,000 ppm, O_2 = 3%. SO_2 = 1,000 (when used), H_20 = 5% (when used) and N_2 = balance. Total flowrate = 500 ml/min. Catalyst amount = 0.4 g.

Figure 27. NO conversion (to N_2) in the NO + O_2 + C_2H_4 reaction over Cu^{2+} ion exchanged TiO_2-pillared clay, with an without SO_2 (500 ppm) and H_2O (5% vol.). NO = 1,000 ppm, C_2H_4 = 250 ppm, O_2 = 2%, catalyst = 0.5 g, N_2 = balance, total flowrate = 150 cc/min. The data of Iwamoto et al. (7,27) on Cu-ZSM-5 catalyst are included for a direct companson. Identical experimental conditions were used.

Figure 28. Promoting effect of Ce on Cu^{2+} exchanged TiO_2 pillared clay in the C_2H_4 SCR reaction. Reaction conditions: NO = 1,000 ppm, C_2H_4 = 250 ppm, O_2 = 2%, catalyst = 0.5 g, total flowrate = 150 cc/min. Amount of dopant = 0.5% (wt.) Ce_2O_3.

Figure 26 NO Conversion On Fe-TI-Bentonite

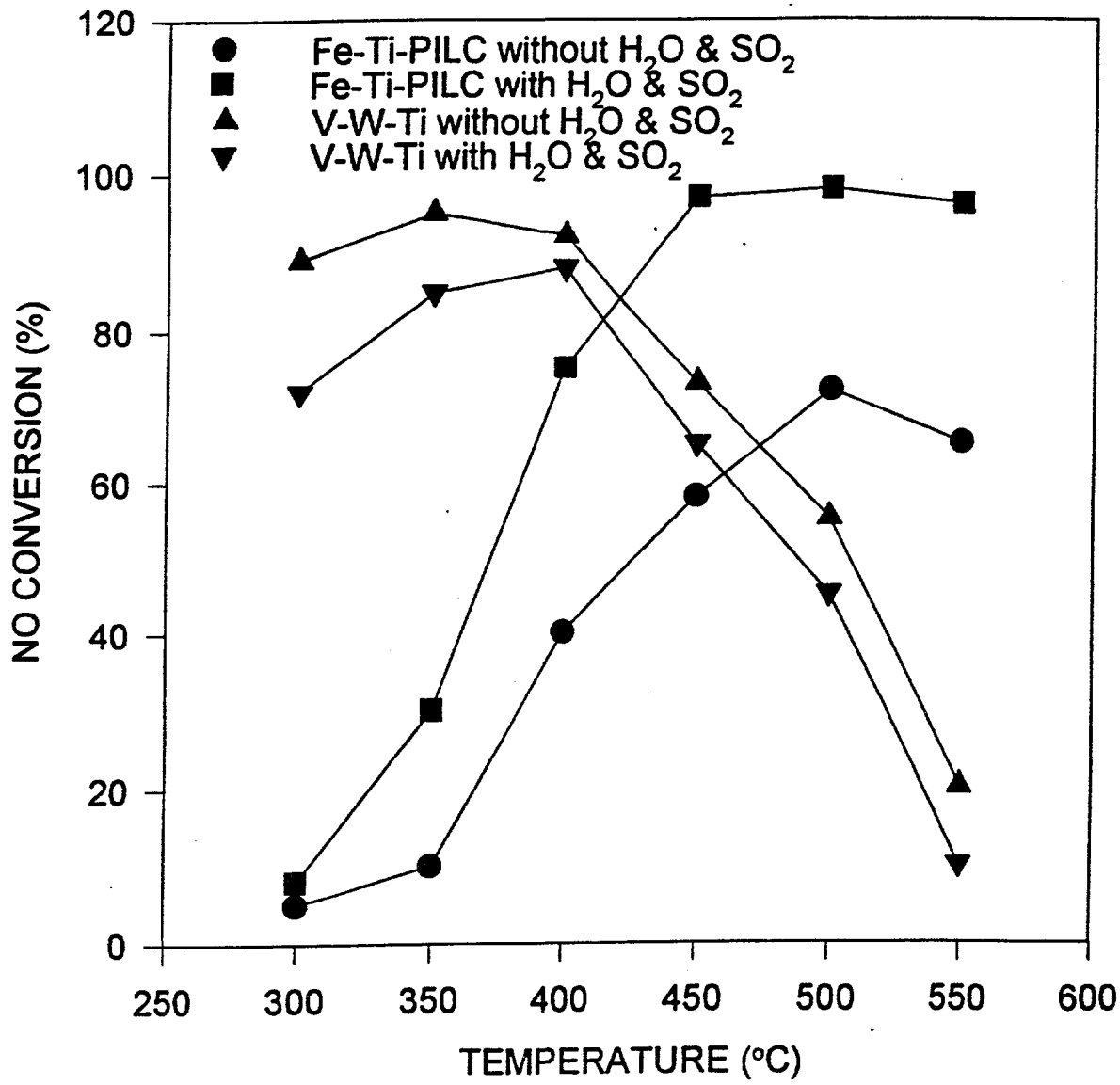

Figure 27

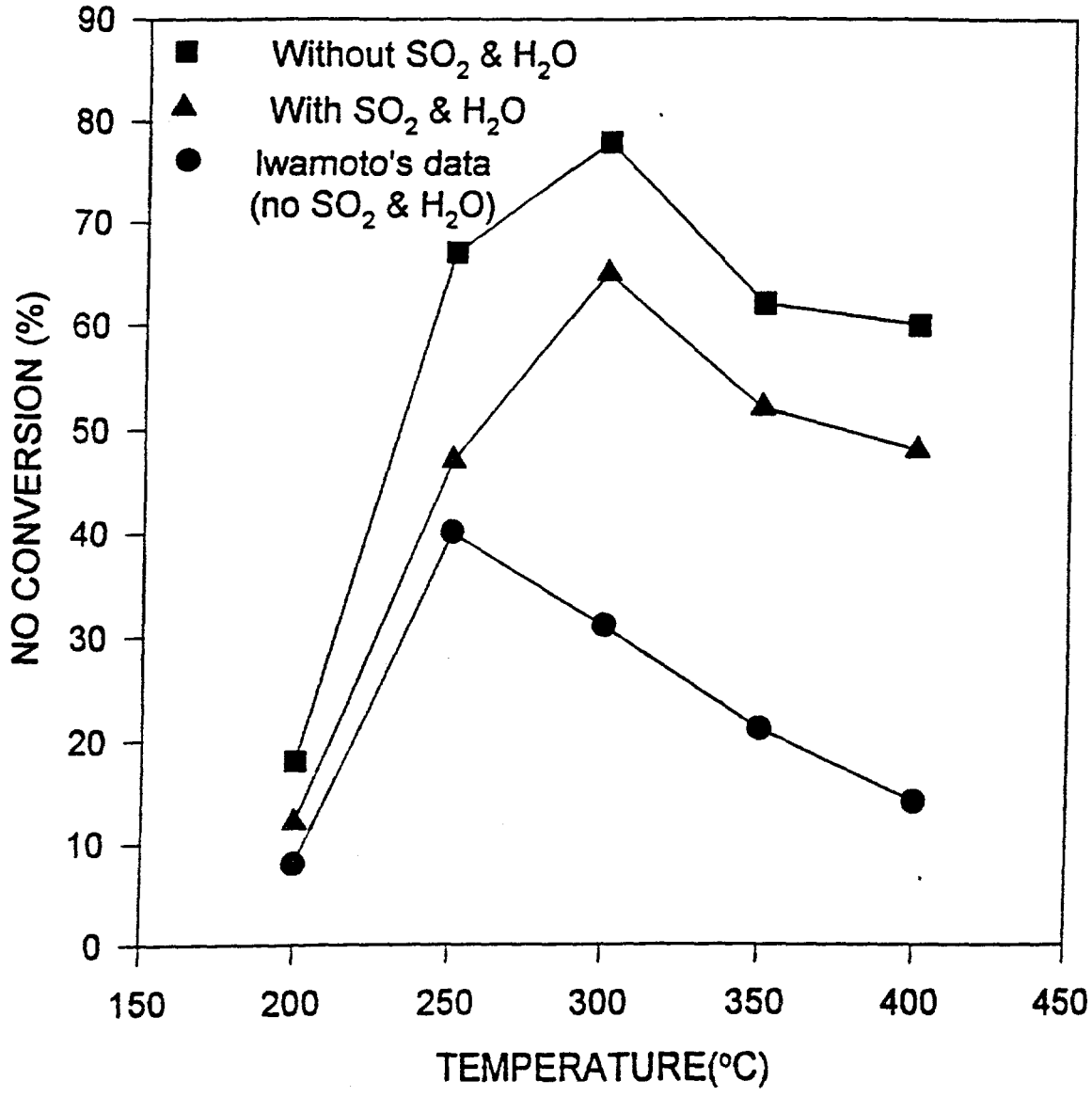
Without SO_2 & H_2O
With SO_2 & H_2O
Iwamoto's data
(no SO_2 & H_2O)
NO CONVERSION (%)
TEMPERATURE(°C)
0
10
20
30
40
50
60
70
80
90
150
200
250
300
350
400
450

Figure 28

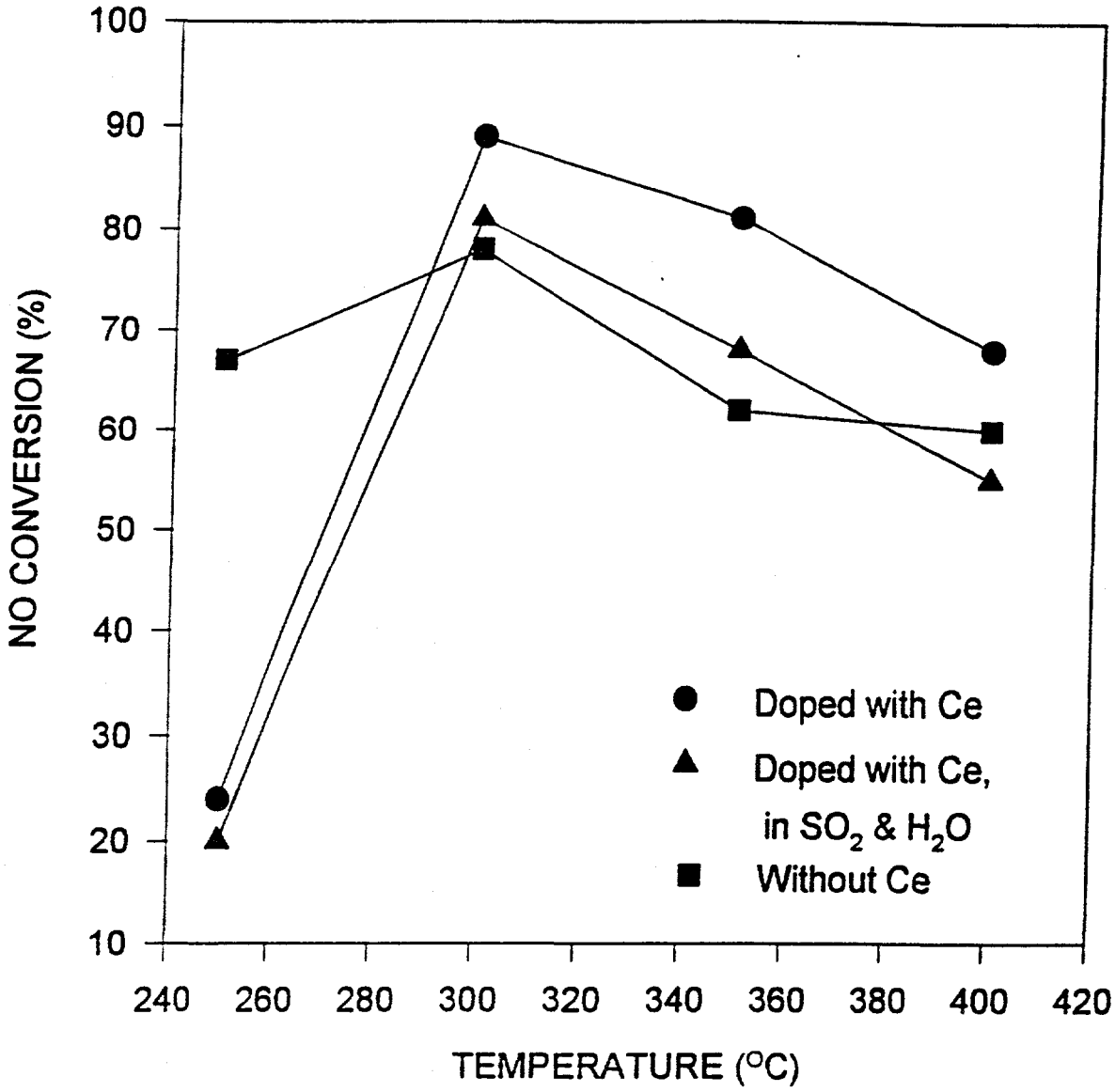
100
90
80
70
60
50
40
30
20
10
NO CONVERSION (%)
240
260
280
300
320
340
360
380
400
420
TEMPERATURE (°C)
Doped with Ce
Doped with Ce, in SO2 & H2O
Without Ce